Experimental constraints on volatile abundances in arc magmas and their implications for degassing processes

B. SCAILLET & M. PICHAVANT

ISTO-CNRS, UMR 6113, 1A rue de la Férollerie, 45071, Orléans Cedex 02, France.

Abstract: Recent phase equilibrium studies, combined with analytical and petrological data, provide rigorous constraints on the pre-eruptive P–T–fH_2O–fO_2–fS_2–fCO_2 conditions of silicic to mafic arc magmas. Pre-eruptive melts show a broad negative correlation between temperature and melt H_2O contents. Pre-eruptive melt S contents cluster around 100 ppm in residual rhyolitic liquids of silicic to andesitic magmas, and range up to 5000 ppm in more mafic ones. For the entire compositional spectrum, melt sulphur contents are almost independent of prevailing fO_2. In contrast, they are positively correlated to fS_2, in agreement with experimental observations. Using these intensive constraints, the composition of coexisting fluid phases has been modelled through a MRK equation of state. Pre-eruptive fluids in silicic to andesitic magmas have XH_2O (mole fraction of H_2O) in the range 0.65–0.95. XH_2O decreases as pressure increases, whereas XCO_2 increases up to 0.2–0.3. Pre-eruptive fluids in hydrous mafic arc magmas, such as high-alumina basalts, generally have similar mole fractions of H_2O and CO_2 at mid-crustal levels, with XH_2O increasing only for magmas stored at shallow levels in the crust (<1 kbar). The sulphur content of the fluid phase ranges from 0.12 up to 6.4 wt% in both mafic and silicic magmas. For silicic magmas coexisting with 1–5 wt% fluid, this implies that more than 90% of the melt+fluid mass of sulphur is stored in the fluid. Calculated partition coefficients of S between fluid and melt range from 17 up to 467 in silicic to andesitic magmas, tending to be lower at low fO_2, although exceptions to this trend exist. For mafic compositions, the sulphur partition coefficient is constant at around 20. The composition of both melt and coexisting fluid phases under pre-eruptive conditions shows marked differences. For all compositions, pre-eruptive fluids have higher C/S and lower H/C atomic ratios than coexisting melts. Comparison between volcanic gas and pre-eruptive fluid compositions shows good agreement in the high temperature range. However, to reproduce faithfully the compositional field delineated by volcanic gases, silicic to andesitic arc magmas must be fluid-saturated under pre-eruptive conditions, with fluid amounts of at least 1 wt%, whereas mafic compositions require lower amounts of fluid, in the range 0.1–1 wt%. Nevertheless, volcanic gases colder than 700 °C are generally too H_2O-rich and S-poor to have been in equilibrium with silicic to andesitic magmas under pre-eruptive conditions, which suggests that such gases probably contain a substantial contribution from meteoric or hydrothermal water.

Introduction

Understanding how water and sulphur supply by magmas may have varied through geological times, as well as identifying the factors that control the abundances of these species in modern and ancient magmas, has implications for fundamental geological processes, such as the long-term geochemical cycles of these elements or the origin and evolution of the atmosphere. On a shorter observational time-scale, which is of more direct relevance to humankind, water and sulphur are among the most important climate forcing species released by volcanic activity worldwide. In particular, sulphur-rich eruptions, such as El Chichón in 1982 or Mount Pinatubo in 1991, have illustrated how volcanic events of even moderate magnitude may affect the Earth's climate on a global scale (Robock 2000; Blake, 2003, Chapter 22). Quantifying the water and sulphur budgets released by arc magmas during the recent past (e.g. Palais & Sigurdsson 1989; Zielinski 1995) has thus become an important aspect of studies attempting to unravel factors affecting secular climate trends based on climate proxies such as ice-core records (Robock 2000). Understanding the behaviour of these two species in magmatic systems is also fundamental from the perspective of volcanic hazard assessment. It has long been known that because arc magmas are water rich they may erupt explosively. The determination of pre-eruptive magma water

From: OPPENHEIMER, C., PYLE, D.M. & BARCLAY, J. (eds) *Volcanic Degassing*. Geological Society, London, Special Publications, 213, 23–52. 0305–8719/03/$15.00

contents is clearly one, although not the only, vital parameter that needs to be constrained in order to predict the eruptive behaviour of volcanoes. Sulphur contributes little to the eruption explosivity, because its abundance is one to two orders of magnitude lower than that of water. However, although minor, this species plays a central role in the monitoring of active volcanoes because it is easily measured with remote sensing tools and thus offers a potential insight into degassing mechanisms occurring at depth (e.g. Watson *et al.* 2000; McGonigle & Oppenheimer, 2003, Chapter 9). Monitoring of SO_2 fluxes of active volcanoes has yielded promising results for the forecast of volcanic eruptions, such as for the Galeras volcano, where SO_2 fluctuations could be correlated with the seismicity associated with magma ascent (Fischer *et al.* 1994). Correctly interpreting volatile degassing in terms of pre-eruptive signals, however, depends on our knowledge of volatile solubilities and diffusivities in silicate melts and their dependence on pressure, temperature and melt composition. It has been one of the main goals of experimental petrology to place narrow constraints on these critical parameters, as demonstrated by numerous studies over the past 18 years (Rutherford *et al.* 1985; Johnson & Rutherford 1989; Rutherford & Devine 1988, 1996; Luhr 1990; Martel *et al.* 1998, 1999; Scaillet & Evans 1999; Scaillet & Macdonald 2001), as well as to establish empirical or thermodynamical models describing the volatile solubilities in silicate melts (e.g. Silver & Stolper 1985; Dixon *et al.* 1995; Zhang 1999; Clemente *et al.* 2003; Moretti *et al.*, 2003, Chapter 6).

Volatiles released either passively or explosively by volcanoes presumably derive from various depths or structural levels where storage and partial degassing of magma bodies take place. Although the exact geometry and size of these bodies remain poorly constrained, and certainly vary between each volcano, there exists usually one upper-crustal reservoir where magma accumulation rates are high enough to build a sizeable body in which differentiation, mixing, degassing and cooling can take place. This reservoir is usually the main source of the erupted material where part, if not most, of the volatiles to be expelled are stored. The fluid/volatile contents of the upper reaches in the plumbing system may be due to the intrinsically volatile-rich nature of the emplaced magma, but also to the fact that, because most volatiles have high solubilities in silicate melts at high pressures, magma bodies in the upper crust may trap volatiles released at deeper levels and thus the plumbing system may act as a channel or channels for volatile degassing. To understand volcanic degassing, it is therefore essential to characterize properly the conditions under which these reservoirs evolve – conditions that correspond with the starting point of any eruptive event.

In this report, we first review recent advances concerning our understanding of sulphur solubility in silicate melts, and its dependence on T, fO_2 and fS_2. We then discuss the pre-eruption P, T, melt H_2O, CO_2 and S values and the corresponding volatile fugacities of well-characterized arc-magmas, as constrained by phase equilibrium, melt inclusion and petrological data, building upon previous reviews (Johnson *et al.* 1994; Scaillet *et al.* 1998*a*, *b*). These constraints are used to derive, from thermodynamic calculations, the composition of the fluid phase that may coexist with the magma at depth before an eruption starts. We finally compare these fluid compositions against high-temperature volcanic gases collected at open vents of well-characterized active volcanoes (e.g. Symonds *et al.* 1994). The rationale is to estimate to what extent fluids coexisting at depth differ from those measured at the vent and, if so, to identify the factors responsible for these differences.

Sulphur solubility and fluid/melt partioning in arc magmas

Solubility

The solubility of sulphur in silicate melt has been extensively reviewed by Carroll & Webster (1994) for both mafic and silicic compositions, and here we focus mostly on the most recent developments in this field. Unlike water, whose solubility depends primarily on pressure, sulphur solubility is controlled by a number of parameters that include melt composition, temperature, fO_2 and fS_2. Until recently, experimental data for silicic systems were available only for the first three parameters. The magnitude of the control exerted by fS_2, although anticipated from experimental studies on dry (1 atmosphere) synthetic and mafic compositions (Carroll and Webster 1994), was virtually unknown. This gap has been filled by recent experimental work in which the interplay between T–fO_2–fS_2 and dissolved sulphur in a silicic magma (rhyolite) has been systematically explored and modelled at 2 kbar (Clemente *et al.* 2003). This study has shown that fS_2 exerts a control on sulphur solubility in hydrous rhyolitic melts, similar in magnitude to that of fO_2. This is illustrated in Figure 1 for a temperature of 930 °C at which most of the data

were acquired, for either sulphide- or sulphate-saturated conditions. Although oxidized conditions need additional constraints in terms of sulphur solubility–fugacity relationships, it can be seen that at any given fixed fS_2, the sulphur solubility exhibits a minimum in the fO_2 range NNO–NNO+1, as shown by many previous studies. For a given T–fO_2, the melt sulphur solubility increases with fS_2, as expected. As a result, the dependence on fO_2 decreases with fS_2 such that at low fS_2 the half bell-shaped curve opens widely to the extent of becoming almost flat (i.e. independent of fO_2). From these experimental data, Clemente *et al.* (2003) have derived the following empirical expression:

$$\log S_{melt} = 0.001\ T(°C) - 0.2567\ (\Delta NNO) + 0.1713\ \Delta FFS + 0.0034\ \Delta NNO\ \Delta FFS \quad (1)$$

where S is the total sulphur concentration in ppm, T temperature in °C, ΔNNO is the log fO_2 referenced to that of the Ni–NiO solid buffer (NNO, calculated after Chou 1987), and ΔFFS is the log fS_2 referenced to the Fe–FeS buffer (calculated after Froese and Gunter 1976). The main limitations of equation 1 are that it has been calibrated only for metaluminous rhyolites saturated with H–O–S fluids, and that the effect of pressure remains to be determined. It is, however, the only model yet available and serves as a useful starting point for the determination of fluid phase composition coexisting at depth, as shown below.

For mafic melt compositions there is as yet no calibrated model for hydrous and oxidizing conditions, which characterize most arc basalts. The only solubility model available for now is that of Wallace and Carmichael (1992), and it has been calibrated on sulphide-saturated and nominally dry compositions up to NNO. In this report we have used a simple empirical model based on the data for MORB glasses of Wallace and Carmichael (1992). To calculate either the melt S ppm or log fS_2, the following polynomial fits have been used:

$$\log fS_2 = -3.9829 + 3.7022\times10^{-2}\ (S_{ppm}) - 1.083\times10^{-6}\ (S_{ppm})^2 + 9.3232\times10^{-11}\ (S_{ppm})^3 \quad (2)$$

and,

$$\log S_{ppm} = 3.2211 + 2.0928\ (\log fS_2) + 9.5397\times10^{-2}\ (\log fS_2)^2 + 3.5864\times10^{-2}\ (\log fS_2)^3 \quad (3)$$

where S_{ppm} is the melt S content in ppm. This model is a mere extension toward oxidizing conditions of the model of Wallace and Carmichael (1992), which is based on the observation that both dry reduced and wet oxidized natural mafic

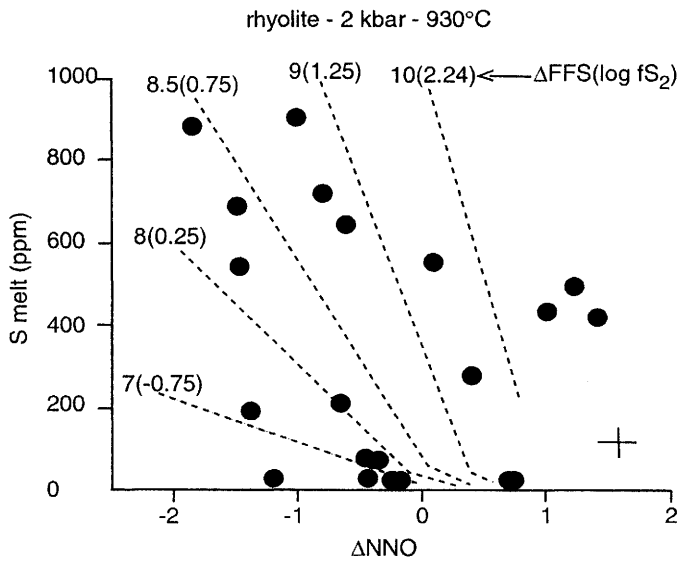

Fig. 1. Sulphur solubility in a sulphide or sulphate-saturated rhyolitic melt at 2 kbar and 930 °C, from Clemente *et al.* (2003). All charges are saturated in either pyrrhotite or anhydrite. Dashed lines represent contours of constant ΔFFS with values of log fS_2 given in parentheses. The cross in the lower right area of the figure represents the average standard deviation (one sigma) of oxygen fugacity (fO_2) and melt sulphur content (see text) .

melts display a single continuous trend relative to fO_2, with only a very weak dependence on redox conditions (see below). Equation 2 calculates log fS_2 within 0.3 log unit of the values reported by Wallace and Carmichael (1992) while equation 3 yields melt S contents to within 14% of those measured by Wallace and Carmichael (1992).

Partitioning

Interest in the partitioning behaviour of sulphur between melt and fluid has essentially been driven by the 'excess sulphur' problem identified for the 1991 Pinatubo eruptions. The huge SO_2 cloud released by Mount Pinatubo cannot be accounted for by the erupted magma volume, considering its pre-eruptive conditions, which were characterized by a low sulphur content of the melt, as represented by matrix and glass inclusions (Westrich & Gerlach 1992). This rules out melt as the main sulphur reservoir at depth. One explanation, put forward by Westrich and Gerlach (1992), is that the excess sulphur resided mostly in a coexisting vapor phase, which implies S_{fluid}/S_{melt} partitioning of about 700–800 (Gerlach *et al.* 1996). Direct determination of the partition coefficients of sulphur in laboratory experiments has been hindered by back reactions in fluids upon quenching, which prevent preservation of the equilibrium compositions of S-bearing magmatic fluids. So far, only two experimental studies have attempted to determine the partition of sulphur between melt and fluid at high P and T. Both used a mass-balance approach where only the S-bearing condensed phases have their sulphur content determined, whereas that of the fluid was calculated by difference (Scaillet *et al.* 1998*b*; Keppler 1999). Both studies have found that under certain conditions there is indeed a strong preferential partitioning of sulphur in favour of the fluid, yet the defined conditions are different between the two studies: Keppler (1999) found sulphur-enriched fluid under low fO_2, while Scaillet *et al.* (1998b) found the opposite. It has to be stressed that this difference is not due to a particular experimental procedure or to an analytical problem. Instead, the reason lies in the different bulk compositions on which the experiments were carried out. Keppler (1999) used a Ca- and Fe-free haplogranite melt composition, while Scaillet *et al.* (1998b) worked with the dacite from the Mount Pinatubo 1991 eruption. The haplogranite compositions used by Keppler (1999) mean that the experimental results are of limited applicability to understanding the behaviour of sulphur in arc-magmas, because the crystallization of S-bearing phases such as anhydrite or pyrrhotite cannot be taken into account. The fO_2 dependence of the partition coefficient obtained by Keppler (1999) must be related to the contrasted solubilities of H_2S and SO_2 fluid species in hydrous Fe and Ca-free silicic melts, and suggests that H_2S is less soluble than SO_2. The experiments of Scaillet *et al.* (1998*b*) have shown that in Fe- and Ca-bearing magmas, part of the sulphur is being locked up by either pyrrhotite or anhydrite. The great affinity of iron and sulphur under reduced conditions results in most sulphur being stored in pyrrhotite and little being available for the fluid phase. Extensive sulphide precipitation makes the coexisting iron-bearing silicate phases (pyroxenes, amphiboles, biotite) becoming richer in magnesium. In contrast, when anhydrite is stable, although this mineral also holds a significant amount of sulphur, its modal proportion is lower than that of pyrrhotite, hence there is more sulphur available for the fluid and melt phases. At low temperatures where the sulphur solubility of silicate melts is low, sulphur resides primarily in the fluid phase. Scaillet *et al.* (1998*b*) suggested that the lower modal amounts of anhydrite relative to pyrrhotite are due to the fact that calcium needed for anhydrite crystallization in hydrous magmas is limited due to plagioclase and hornblende precipitation. For mafic compositions, there are no experimental constraints on the partitioning behaviour of sulphur between fluid and melt.

Pre-eruptive conditions

Rhyolitic to andesitic compositions

Johnson *et al.* (1994) and Scaillet *et al.* (1998a) have reviewed the available evidence for the pre-eruptive conditions determined for several arc-volcanoes using a variety of approaches including phase equilibria, melt inclusion and mineral equilibria (Fe–Ti oxides). In this work we use the database of Scaillet *et al.* (1998a), excluding all non arc-magma compositions, to which we have added the results of recent phase equilibrium or analytical works (Katmai: Coombs & Gardner 2001; Minoan: Cottrell *et al.* 1999; Michaud *et al.* 2000; Unzen: Sato *et al.* 1999). In the case of chemically zoned eruptions (e.g. Katmai, Bishop, Krakatau, Minoan) we restrict the analysis to volcanic ejecta believed to represent the top portion, or first tapped part, of the magmatic reservoir, except for the Pine Grove where the deepest possible magma (i.e. the CO_2 rich part) has been used in an effort to shed light on the lowest regions of the plumbing system. In the most favourable cases, the combination of phase equilibrium, melt inclusion, and oxide thermo-

barometry constraints generally allows us to define the pre-eruption temperature to within ±30 °C, melt H_2O content to ±0.5 wt% and fO_2 to ±0.3 log unit. Good examples include the recent eruptions of Mount St Helens, Mount Pelée, Montserrat and Mount Pinatubo. Pressure is the least well-constrained parameter. The spatial resolution of geophysical data (e.g. seismic, gravimetric, magnetotelluric methods) is often too low to image accurately magma bodies that are only a few km across, which is the expected size for the most frequent type of eruptions involving up to a few km^3 of erupted material. Most pressures of magma storage are derived from phase equilibrium constraints (Pinatubo, St Helens, El Chichón, Fish Canyon, Mount Pelée, Montserrat, Mount Unzen, Katmai, and Minoan), coupled, when available, with seismic data (e.g. Pinatubo, St Helens). Melt inclusion barometry can also help to constrain pressures of magma storage, assuming fluid saturation (Wallace *et al.* 1995). Such constraints have been used for the Bishop and Pine Grove eruptions. For other eruptions (Krakatau, Taupo, Toba, Santa Maria) lacking seismic or phase equilibrium constraints on depth of the magma reservoir, the pressure of magma storage before eruption has been assumed to be at 2–3 kbar for amphibole-bearing magmas (Toba, Taupo, Santa Maria) and 1.2 kbar for magmas lacking this phase (Krakatau). We stress, however, that these amphibole-based constraints are only crude estimates that need refinement. Based on available experimental data, there is a general consensus that amphibole presence in andesitic–dacitic magmas requires a minimum of 1–1.5 kbar (e.g. Rutherford & Hill 1993), but recent work has established that amphibole may persist down to 500 bars in some dacitic groundmasses (Sato *et al.* 1999), while in others amphibole crystallization on the liquidus requires at least 4 kbar (Martel *et al.* 1999). The broad chemical similarities of the rocks in these experimental studies show that the compositional control of amphibole stability in andesitic–dacitic magmas is subtle, and additional experimental work is required before amphibole geobarometry can be of general, as well as precise, use in arc settings.

The critical pre-eruption parameters are listed in Table 1, together with the melt atomic C/S, H/S and H/C ratios. Most volcanoes have their upper crustal reservoir, which may correspond with either the top portion of a larger vertical system tapped during eruption (e.g. Pichavant *et al.* 2002*a*) or to a single isolated magma body with limited vertical dimensions, at a pressure of 2 ± 1 kbar. Pre-eruptive melt water contents range from 4 to 7 wt%, temperatures between 675 and 900 °C, and fO_2 between NNO and NNO+2. A general inverse correlation exists between T and H_2O, such that the drier the magma, the hotter it is. This trend may, in part, reflect the fact that magmatic differentiation is accompanied by a decrease in temperature and a concentration of water in the residual melt (Fig. 2, see also Scaillet *et al.* 1998*a*). Such a trend does not exist for both the melt CO_2 (calculated as explained below) and S contents, whose abundance seems fairly insensitive to the temperature of magma storage (Fig. 2). In contrast, melt CO_2 contents show a broad positive dependence on pressure, reaching a maximum at around 500 ppm for magmas stored in the middle crust (Pine Grove) (Fig. 3). Melt S concentrations display a remarkably flat trend over nearly two log units of fO_2 (Fig. 3), most magmas having S concentrations at around 100 ppm under pre-eruption conditions. The lack of clear dependence between melt S concentration and fO_2 suggests that variations in fO_2 do not significantly affect the melt sulphur in silicic to andesitic arc magmas, at least in the upper portions of the storage zone. In contrast, there is a gentle positive correlation between melt S concentration and fS_2 (Fig. 3). Overall, calculated fS_2 ranges from 10^{-5} up to a few bars, in agreement with previous work (Whitney 1984).

Basaltic compositions

The number and quality of quantitative constraints on pre-eruptive conditions for mafic systems are more limited than those for silicic systems. The main reason is that, owing to the strong negative dP/dT slopes of crystallizing phases in H_2O-bearing magmas coupled to the low viscosity of hydrous mafic melts, mafic arc-magmas rarely erupt without extensive crystallization. This seriously hampers conventional petrological laboratory studies. Over the last decade, however, major advances have been made (see Johnson *et al.* 1994), largely thanks to experimental studies (e.g. Sisson & Grove 1993*a*, *b*; Pichavant *et al.* 2002*a*, *b*) or analytical work on melt inclusions (e.g. Sisson & Layne 1993; Sobolev & Chaussidon 1996; Roggensack *et al.* 1997; Luhr 2001; Roggensack 2001). It is important to distinguish MgO-rich arc basalts from MgO-poor ones with which we will be primarily concerned in this study. The former correspond with the most primitive type (i.e. mantle-derived) of magma found in arc settings, albeit very seldom for the reasons just given, and which last equilibrated with mantle rocks. Recent phase equilibria have shown that such primary arc magmas, with MgO contents higher than 10 wt%, have melt H_2O contents of around 2 wt%

Table 1. *Pre-eruptive volatile fugacities of arc magmas*

Eruption	SiO_{2melt} (wt%)	P_{tot} (bar)	P min[1] (bar)	T (°C)	ΔNNO[2]	Log fO_2	H_2O[3] wt%	fH_2O[4] (bar)	fH_2[5] (bar)	S melt (ppm)	fS_2[6] (bar)	fS_2–Po[7] (bar)	fCO_2[8] (bar)	CO_2[9] (ppm)	C/S	H/S	H/C
Silicic to andesitic compositions																	
Pinatubo	78	2200	2150	760	1.70	–12.98	6.0	1517	1.06	75	0.06435	–	201	67	0.32	1422	4378
Bishop	77	1800	1800	720	0.20	–15.46	5.4	1177	4.53	100	0.00163	0.00200	100	37	0.13	967	7188
Toba	77	3000	2000	730	0.39	–14.97	5.7	1529	4.49	–	–	0.00088	1817	454	2.01	1236	614
St Helens	74	2200	1450	930	1.18	–10.10	4.6	1334	2.03	68	0.12747	0.40000	945	329	1.76	1203	684
Krakatau	72	1200	1100	890	1.20	–10.83	4.0	958	1.42	200	47.3446	0.40000	80	36	0.07	356	5432
El Chichón	70	2000	1600	800	1.00	–12.79	5.0	1289	2.13	150	0.97917	0.07330	466	162	0.39	593	1509
Fish Canyon	77	2400	1550	760	1.70	–12.97	5.0	1231	0.85	–	–	1.60000	1135	351	0.95	658	696
Mt Pelée	75	2000	1900	875	0.60	–11.68	5.5	1593	4.48	100	–	0.09844	120	44	0.16	978	6111
Montserrat	76	1400	1400	850	1.00	–11.78	4.7	1143	2.04	100	0.09689	–	17	8	0.03	995	28 722
Mt Unzen	77	1100	1050	850	1.60	–11.19	4.0	872	0.79	50	0.03357	–	84	40	0.29	1422	4889
Taupo	76	2000	1450	800	0.00	–13.79	5.0	1245	6.50	44	3.7×10^{-5}	–	575	205	1.69	2020	1192
Pine Grove	76	4050	4050	675	0.79	–15.95	7.0	2176	3.53	60	8.8×10^{-5}	–	2973	491	2.98	2074	697
Katmai	76	1000	1000	825	0.25	–13.05	4.0	831	3.49	65	0.00158	0. 0316	25	12	0.07	1094	16296
Santa Maria	74	2000	1250	833	–0.50	–13.60	4.2	1032	9.88	198	0.09139	–	920	330	0.61	380	627
Minoan	74	2300	2150	825	0.50	–12.75	6.0	1747	5.18	90	0.01660	–	169	55	0.22	1185	5333
Basaltic compositions																	
Parent	48	–	5200	1050	1.50	–7.80	6.0	3700	3.90	3074	7.0000	–	5101	1007	0.24	69	291
Cerro Negro	49	–	3000	1050	1.50	–7.88	3.8	1400	1.60	800	0.0100	–	2810	881	0.80	169	211
Cerro Negro	48	–	3000	1050	1.50	–7.88	4.2	1700	2.00	1300	0.2100	–	2071	650	0.37	115	316
Cerro Negro	55	–	2300	1050	1.50	–7.90	4.2	1550	1.80	800	0.0100	–	927	337	0.31	187	609
Cerro Negro	52	–	1600	1050	1.50	–7.93	3.0	1050	1.00	600	0.0045	–	865	364	0.43	172	403
Cerro Negro	51	–	800	1050	1.50	–7.96	2.8	700	0.90	300	0.0010	–	63	32	0.08	339	4431

[1]Minimum pressure at which the chemical equilibrium condition is satisfied in a C–O–H–S fluid using the tabulated T, fO_2, fH_2O and fS_2 values.
[2]log fO_2 referenced to the fO_2 value of the Ni–NiO solid buffer (Chou 1987) at the given P and T.
[3]H_2O in melt determined by phase equilibrium, FTIR or VBD approaches. See Scaillet *et al.* (1998*a*, *b*) for sources, and also text.
[4]For silicic to andesitic magmas the fH_2O have been calculated using the melt H_2O content and the model of Zhang (1999). For basaltic compositions, the model of Dixon *et al.* (1995) has been used, with thermodynamic parameters as listed in Holloway & Blank (1994).
[5]fH_2 calculated from the dissociation equilibrium of water, using fO_2, fH_2O and thermodynamic data from Robie *et al.* (1978).
[6]fS_2 calculated using the empirical model of Clemente *et al.* (2003) for silicic to andesitic compositions or equations (2) and (3) for basaltic compositions derived from the data-set of Wallace & Carmichael (1992).
[7]fS_2 calculated using the pyrrhotite composition and the thermodynamic model of Toulmin & Barton (1964) implemented by Froese and Gunter (1976). For Mount Pelée, the pyrrhotite composition used to calculate fS_2 is from Martel (1996).
[8]For silicic to andesitic compositions, fCO_2 have been calculated using the MRK equation of state of Holloway (1977), modified by Flowers (1979), in the C–O–H–S system using listed P, T, fH_2, fH_2O and fS_2 values. When there are two fS_2 available, the calculation has been done using the one corresponding to the pyrrhotite composition. For basaltic compositions, fCO_2 is calculated using the melt CO_2 content and the model of Dixon *et al.* (1995).
[9]For silicic to andesitic compositions, melt CO_2 contents have been calculated using the thermodynamical model of Blank *et al.* (1993) and Holloway and Blank (1994). For basaltic compositions, melt CO_2 contents are similar to those measured by Roggensack *et al.* (1997) on Cerro Negro melt inclusions. Note that only melt inclusions where both H_2O and S were also known have been taken into account.

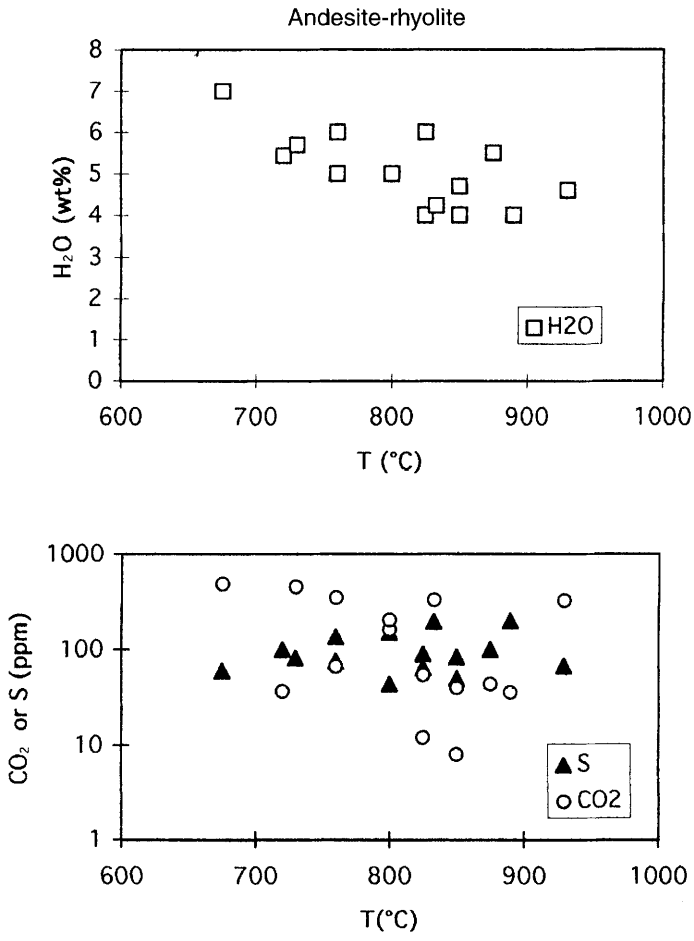

Fig. 2. Variation of the pre-eruptive melt H_2O, CO_2, and S contents with temperature in silicic to andesitic magmas. The SiO_2 content of the melts ranges from 70 up to 78 wt%.

or higher (Fig. 4) and are extracted from the mantle wedge at temperatures around 1200 °C (Pichavant *et al.* 2002*b*).

Arc basalts having MgO contents significantly lower than 7–8 wt% are widely believed to be derivative products of such primary mantle melts (e.g. Sisson & Grove 1993*a*, *b*; Pichavant *et al.* 2002*a*). In particular, high-alumina basalts (HABs), which commonly occur in convergent zones, can be derived by fractionation of these primitive, almost picritic, basalts (e.g. Sisson & Grove 1993*b*). If this scenario is of general validity, because of the largely incompatible behaviour of water in such systems, the melt H_2O contents of HABs must be substantially higher than 1–2 wt%. Both melt inclusion and phase equilibrium constraints have indeed shown that, in many instances, the melt H_2O content of such magmas at depth is at least 4 wt%, and concentrations as high as 8–9 wt% have been reported (Fig. 4) (Sisson & Grove 1993b; Pichavant *et al.* 2002*a*). There are no direct constraints on temperature, but experimental data show that high-Mg HAB (with 7–8 wt% MgO) are produced within a temperature range 1100–1200 °C from the crystallization of primitive basalts, while the dominant low-Mg HAB type (with 3–5 wt% MgO) is, in turn, produced by crystallization of high-Mg HABs in the temperature range 1000–1100 °C (all under hydrous conditions as required by phase assemblages and compositions). Although the available data show that mafic arc melts display a negative correlation between melt H_2O content and temperature,

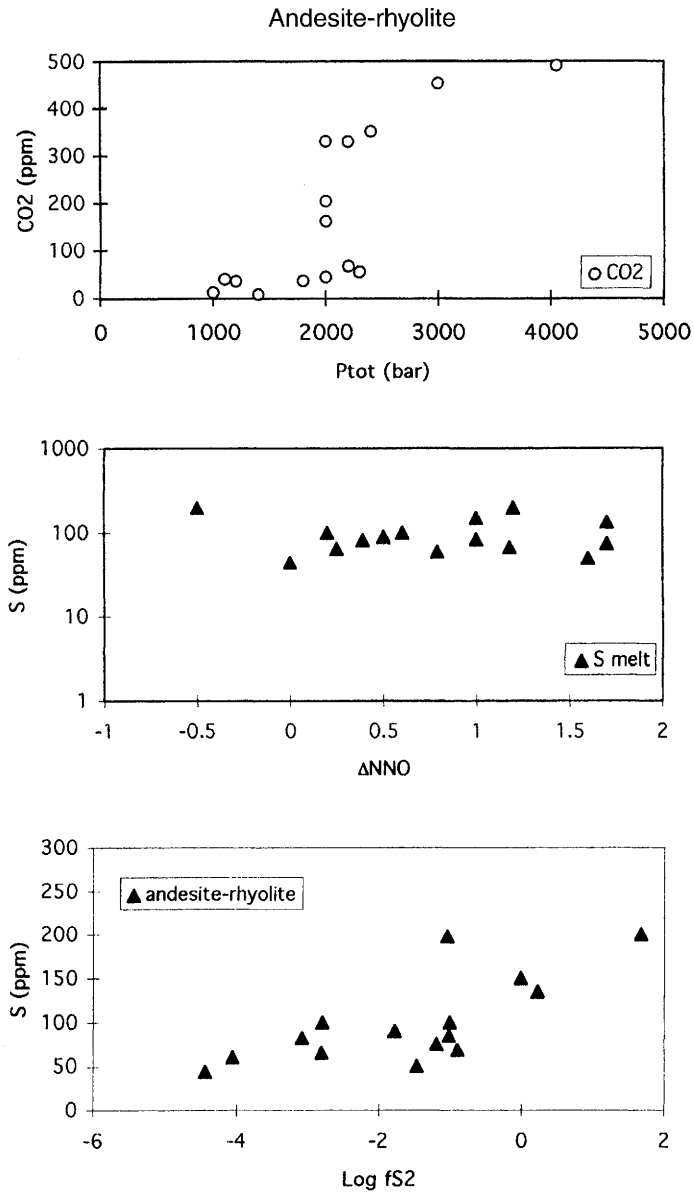

Fig. 3. Variation of pre-eruptive melt CO_2 and S contents with pressure (CO_2), fO_2 (S) and fS_2 (S) in silicic to andesitic magmas.

additional work is needed to confirm this trend. The mafic trend does not join that defined by silicic to intermediate magmas, both groups having clearly distinct fields in the T–H_2O projection (Fig. 4). The few mafic melt inclusions analysed for CO_2 (Roggensack *et al.* 1997; Sisson & Bronto 1998; Luhr 2001; Roggensack 2001) point to pre-eruptive melt CO_2 contents of up to 1000 ppm, with a corresponding H_2O content of up to 6 wt% (Table 1), in agreement with the phase equilibrium constraints detailed above. This indicates that the pressure of magma storage may be as high as 5–6 kbar (Table 1). Although the level of uncertainty is high, since these HAB are parental to most andesite–dacite arc series, they must lie in the deeper part of the plumbing system, which implies pressures in excess of 2–3 kbar, although some may cross-cut

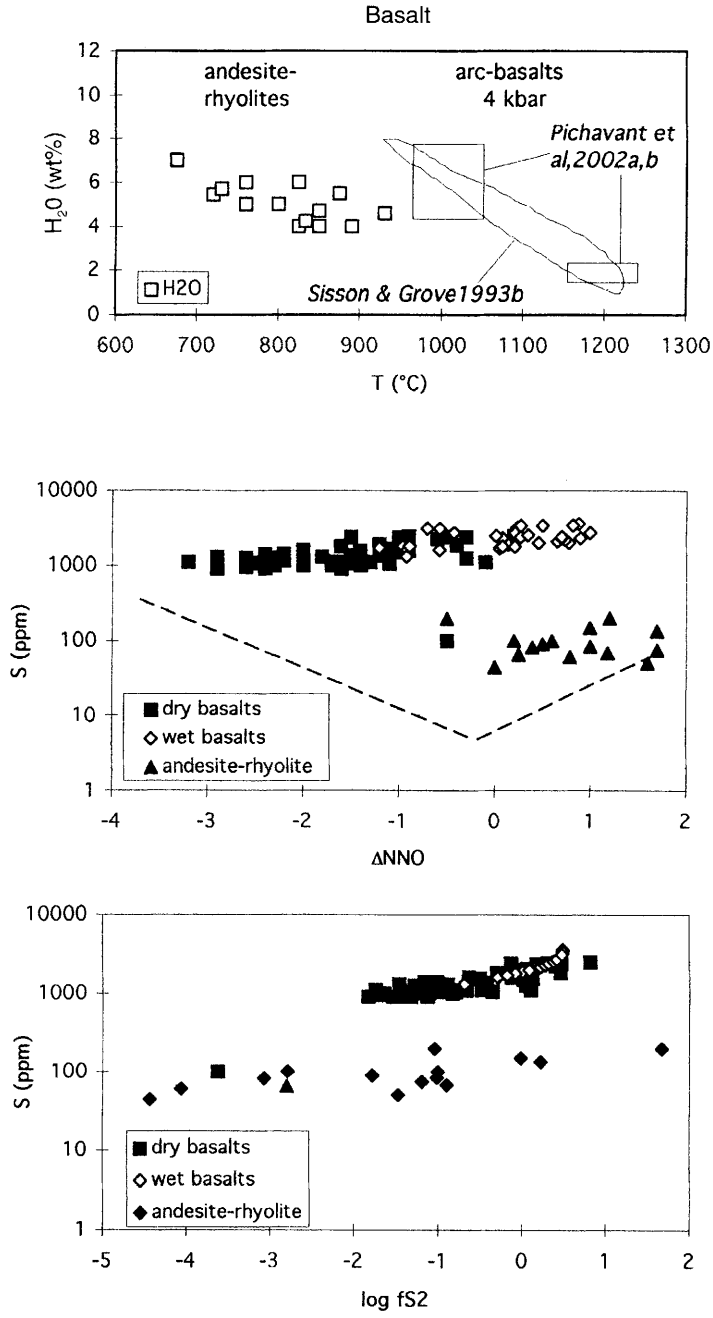

Fig. 4. Variation of pre-eruptive melt H_2O and S contents with temperature, fO_2 and fS_2 in basaltic arc magmas (wet basalts), compared to arc rhyolites–dacites–andesites (Fig. 2) and MORB type basalts (dry basalts) (Wallace & Carmichael 1992). In the T–H_2O diagram, the field corresponds to plagioclase–liquid equilibrium constraints (Sisson & Grove 1993b), while the two boxes are from phase equilibrium constraints on Lesser Antilles arc basalts (Pichavant *et al.* 2002*a*, *b*). In the S–ΔNNO plot, the dashed line represents the sulphur solubility of a dry basaltic melt equilibrated with H–C–O–S fluids at 1 bar and 1250 °C, under various fO_2 (see Carroll & Webster 1994). The sulphur fugacities of arc basalts have been calculated using equation 2 and data from Métrich & Clocchiatti (1996).

the silicic reservoirs. With respect to the redox state of these mafic magmas, there are again very few direct constraints, but experimentally produced liquid lines of descent broadly match observed calc-alkaline trends, in particular their low FeO_{tot}/MgO ratio, provided that the fO_2 is higher than NNO (Sisson & Grove 1993*a*; Pichavant *et al.* 2002*a*). Both melt and natural mineral compositions suggest that the relatively deep part of some magma reservoirs may be more oxidized than their upper part, with fO_2 in the range NNO+1 to NNO+2, or even higher (Pichavant *et al.* 2002*a*). Here we have adopted a constant value of NNO+1.5 (Table 1).

The sulphur content of mafic arc melts is known primarily from melt-inclusion studies (e.g. Métrich & Clocchiatti 1996; Roggensack *et al.* 1997; Sisson & Bronto 1998; Métrich *et al.* 1999; Luhr 2001). Mafic arc magmas consistently display S contents similar to or higher than those of mid-ocean ridge basalts (MORB), despite the fact that both types of magma differ widely in their redox states. In fact, the hydrous oxidized mafic arc magmas extend toward high fO_2 the trend defined by MORB melts (Fig. 4). Although there is a slight positive increase in melt S content with fO_2, the redox trend is again remarkably flat over more than 4 log units. This is in spectacular contrast to the laboratory behaviour of basaltic melt compositions undersaturated in sulphide, which shows a prominent solubility minimum around NNO (Fig. 4). As for the H_2O–T projection, there is no overlap between the mafic and silicic–andesitic data-sets in the S–log fO_2 diagram. This gap, however, is mainly due to the preference given in this work to consider only the most fractionated, i.e. with rhyolitic residual melt, magma of a given eruption. For instance, at Krakatau, andesitic melt inclusions have sulphur contents up to 1186 ppm (Mandeville *et al.* 1996).

Composition of the pre-eruptive fluids

Method

The composition of the coexisting fluid phase has been calculated using the modified Redlich–Kwong equation of state of Holloway (1977), as modified by Flowers (1979). Calculations have been performed in the C–O–H–S system, taking into account the following species: H_2O, H_2, CO_2, CO, CH_4, SO_2, H_2S, S_2 and O_2. We therefore ignore the contribution of halogens such as F and Cl, basically because the activity–composition relationships (that is, the relation between solubilities and fugacities) of these volatiles in silicate melts are still not well established. Because C–O–H–S bearing species account for more than 95 mol.% of the species in magmatic fluids, this approximation is in most cases justified. By the phase rule we have:

$$v = 2 + C - \varphi \quad (4)$$

where C is the number of constituents (four: C, O, H and S), φ is the number of phases (one: the fluid phase), and v is the degree of freedom (five). If pressure, temperature, and three additional intensive parameters are fixed (i.e. fH_2, fH_2O and fS_2 or fH_2O, fCO_2 and fH_2), the system is invariant and we can calculate the fluid phase composition and the fugacities of all remaining fluid species.

For silicic to andesitic magmas, calculations were performed at the listed pre-eruptive P–T values (Table 1), using as input parameters fH_2O, fH_2 and fS_2. To calculate fH_2O, we use the model of Zhang (1999), together with the melt water content, the anhydrous melt composition and the pre-eruptive P and T. The fH_2 is then calculated knowing fO_2 and fH_2O as calculated above, using the dissociation equilibrium of water (Robie *et al.* 1979). For calculating fS_2 we use the empirical model of Clemente *et al.* (2003). Also listed is the minimum pressure that is needed in order to meet the chemical equilibrium condition in the fluid phase. In other words, calculating the fluid species fugacities at a pressure lower than this minimum would result in fluid pressures being higher than total pressures. An interesting output of such calculations is the derivation of the fugacities of all C-bearing species, even though none is known. Therefore, for each eruption we can also derive the fCO_2 prevailing in the storage region, assuming the presence of a free fluid phase at depth. From this, the melt CO_2 content can be calculated using the Blank *et al.* (1993) thermodynamic model. In cases where the pre-eruptive melt CO_2 contents are also known from melt inclusion data, we thus have an independent constraint on the choice of the input pressure, which is usually the least constrained parameter.

If the fH_2O for a given melt H_2O content is close to that corresponding with H_2O saturation, then the resulting fluid phase must be very poor in C-bearing and S-bearing species. Alternatively, if the calculated fH_2O at the fixed pressure is far from that required to saturate the melt in H_2O (i.e. a melt with 3 wt% H_2O at 2 kbar, at which the saturation in H_2O requires 6–7 wt% H_2O), then the calculated fluid phase must be richer in C- or S-bearing species. Because in our calculations the S-bearing fugacities are fixed by the input fS_2, it follows that the major source of compositional variation of the calculated fluid

phase concerns the proportions of C-bearing species that in turn arise from uncertainties in total pressure. Basically, for a given P and T and set of fH_2O, fH_2, and fS_2, the fugacities of C-bearing species are calculated so that the sum of partial pressures of each volatile species equals total pressure, as equilibrium demands.

A useful limiting case is when melt inclusions have CO_2 contents below the detection limit of infrared spectroscopy (e.g. Montserrat and Mount Pelée), which is in the range 10–20 ppm. Because there will always be some, even minor, amounts of CO_2 in a magmatic system, this indicates that the pressure of magma storage must be close to that defined by volatile saturation in the H–O–S system with calculated melt CO_2 (or fCO_2) being lower than the FTIR detection limit. For instance, at Mount Pelée the calculation performed at 2 kbar yields a melt CO_2 content of 120 ppm, while analysed melt inclusions yield contents below detection levels (Martel, pers. comm.). Such low CO_2 contents are attained when the total pressure approaches the minimum required for chemical equilibrium, which is around 1.9 kbar for Mount Pelée (Table 1), or only 100 bar lower than the pressure deduced from phase equilibrium considerations. In other words, the assumption of fluid saturation, coupled with thermodynamic calculations of volatile solubilities in both the melt and fluid phases, provides an extremely precise tool for determination of the minimum depth of magma storage. However, given the level of uncertainty attached to the input parameters, it is clear that the fluid compositions calculated in the way outlined above may have large uncertainties (as illustrated below for the Santa Maria 1902 eruption), which could obscure or hamper their comparison with volcanic gas data. Given the assumption that the uncertainty of each given set of parameters is similar between different eruptions, we have applied the approach to as many eruptive events as possible, including those that clearly deserve additional work but which allow us to explore the effect of a given parameter over a broader range (Santa Maria, Taupo). Because the data-set covers a considerable range in P–T–fO_2–fH_2O–fS_2 conditions, the compositional field of the calculated fluids is believed to represent the maximum possible error associated with any specific single event, although for particularly well-constrained eruptions (Pinatubo, Pelée, St Helens, Montserrat, El Chichón) the uncertainty is much smaller.

As stressed above the existing data-set on pre-eruption conditions for mafic compositions is very limited. To calculate the fluid phase composition coexisting with such melts, we have adopted a slightly different strategy from that for silicic to andesitic magmas. We have considered melt inclusion data from Cerro Negro where H_2O, CO_2 and S have been measured (Roggensack *et al.* 1997). From these, fH_2O, fCO_2 have been derived at a fixed temperature at 1050 °C. We use the model of Dixon *et al.* (1995) to calculate fH_2O from the melt H_2O content, and the model of Holloway and Blank (1994) to calculate fCO_2 from the melt CO_2 content. The fO_2 is fixed at NNO+1.5, which permits calculation of fH_2 with fH_2O as outlined above, using the dissociation equilibrium of water. Thus the input parameters are here fH_2O, fCO_2 and fH_2, in addition to T and P. In a similar approach to that used for C-bearing species in silicic to andesitic magmas, the S-bearing species fugacities can be calculated. Knowing fS_2, we can then calculate the melt S content using equation 3, and compare it with measured values. Because there are no independent constraints on the pressure of magma storage, the calculations correspond with the minimum pressure required for chemical equilibrium in the fluid.

The melt inclusions analysed at Cerro Negro record widely different fluid saturation pressures, which range from 0.8 up to 3 kbar (Table 2). Such a dispersion in pressure suggests that the various melt inclusions record magma conditions (and thus fluid conditions if fluid-saturated) last equilibrated at various levels in the upper crust (see for instance Roggensack 2001). In addition to these melt inclusion constraints, we have also calculated the fluid phase composition of a hypothetical mafic melt (termed Parent) having 6 wt% H_2O, 1000 ppm CO_2 and about 3000 ppm of dissolved S (Table 2). The melt H_2O and CO_2 contents are the highest recorded at Cerro Negro, while the S content is within the range of the S concentration of melt inclusions of the Fuego volcano (1700–5200 ppm, Rose *et al.* 1982; Roggensack 2001), and also similar to the maxima analysed in some alkali-rich and oxidized basaltic arc magmas by Métrich & Clocchiatti (1996). These volatile contents imply a saturation pressure of 5.2 kbar, and can be considered to model a deep and presumably less degassed stage for a mafic arc magma. The whole data-set thus spans 5 kbar in saturation pressures and is used to track the evolution of fluid phases coexisting with mafic arc magmas as they rise through the upper crust.

Silicic to andesitic melt compositions

The results of calculations are listed in Table 2. The fluid phases coexisting at depth are all water-rich with mole fractions of H_2O (XH_2O) higher

Table 2. *Pre-eruptive fluid compositions of arc magmas*

Eruption	P_{tot} (bar)	T (°C)	ΔNNO	XH_2O	XH_2	XCO_2	XCH_4	XCO	XSO_2	XH_2S	XS_2	C/S	H/S	H/C	S_{fluid} (wt%)	S_{melt} (ppm)	S_{fluid}/S_{melt}
Silicic to andesitic compositions																	
Pinatubo	2200	760	1.70	0.933	0.00018	0.063	1.5×10^{-10}	1.3×10^{-5}	0.00148	0.00708	1.3×10^{-5}	7	219	30	1.38	75	184
Bishop	1800	720	0.20	0.955	0.00095	0.044	4.3×10^{-7}	9.8×10^{-5}	4.6×10^{-6}	0.00933	3.8×10^{-7}	4	184	44	1.72	100	172
Toba	3000	730	0.39	0.724	0.00049	0.269	5.6×10^{-7}	0.00024	2.7×10^{-6}	0.00309	9.3×10^{-8}	87	471	5	0.40	–	–
St Helens	2200	930	1.18	0.708	0.00048	0.282	8.9×10^{-10}	0.00035	0.00891	0.00871	9.5×10^{-5}	16	81	5	2.17	68	319
Krakatau	1200	890	1.20	0.912	0.00074	0.062	1.8×10^{-10}	6.8×10^{-5}	0.01549	0.01820	0.00022	2	55	30	5.21	200	261
El Chichon	2000	800	1.00	0.832	0.00047	0.162	5.8×10^{-9}	0.00011	0.00059	0.01230	1.6×10^{-5}	13	131	10	1.83	150	122
Fish Canyon	2400	760	1.70	0.708	0.00014	0.263	6.6×10^{-10}	7.2×10^{-5}	0.00631	0.02818	0.00028	8	42	6	4.31	–	–
Mt Pelée	2000	875	0.60	0.933	0.00105	0.048	4.9×10^{-9}	6.9×10^{-5}	0.00068	0.01549	2.3×10^{-5}	3	117	40	2.68	100	266
Montserrat	1400	850	1.00	0.955	0.00079	0.011	1.7×10^{-10}	1.1×10^{-5}	0.00389	0.02344	0.00011	0	71	170	4.67	100	467
Mt Unzen	1100	850	1.60	0.912	0.00045	0.072	5.0×10^{-11}	4.2×10^{-5}	0.00813	0.00447	1.9×10^{-5}	6	145	25	1.99	50	398
Taupo	2000	800	0.00	0.794	0.00145	0.195	6.6×10^{-7}	0.00045	1.3×10^{-6}	0.00085	8.3×10^{-9}	229	1869	8	0.12	44	27
Pine Grove	4050	675	0.79	0.794	0.00018	0.214	2.3×10^{-7}	6×10^{-5}	3.4×10^{-7}	0.00074	4.2×10^{-9}	288	2145	7	0.10	60	17
Katmai	1000	825	0.25	0.955	0.00219	0.024	1.1×10^{-8}	4.4×10^{-5}	9.3×10^{-5}	0.00832	2.0×10^{-6}	3	229	80	1.45	65	223
Santa Maria	2000	833	–0.50	0.646	0.00251	0.295	5.2×10^{6}	0.00182	3.7×10^{-5}	0.05248	2.4×10^{-5}	6	27	5	6.35	198	321
Minoan	2300	825	0.50	0.933	0.00087	0.052	1.7×10^{-8}	5.9×10^{-5}	8.5×10^{-5}	0.00871	2.8×10^{-6}	6	214	36	1.45	90	161
Basaltic compositions																	
Parent	5200	1050	1.50	0.642	0.00027	0.308	2.7×10^{-10}	0.00037	0.04181	0.00840	0.00043	6	26	4	5.82	3074	19
Cerro Negro	3000	1050	1.50	0.517	0.00028	0.476	1.0×10^{-10}	0.00077	0.00551	0.00033	1.7×10^{-6}	82	177	2	0.61	800	8
Cerro Negro	3000	1050	1.50	0. 606	0.00034	0.368	1.2×10^{-10}	0.00056	0.02290	0.00187	3.5×10^{-5}	15	49	3	2.77	1294	21
Cerro Negro	2300	1050	1.50	0.721	0.00044	0.269	6.9×10^{11}	0.00038	0.00855	0.00055	2.6×10^{-6}	30	159	5	1.15	800	15
Cerro Negro	1600	1050	1.50	0.588	0.00042	0.399	3.8×10^{-11}	0.00068	0.01058	0.00032	1.9×10^{6}	37	108	3	1.21	619	20
Cerro Negro	800	1050	1.50	0.911	0.00087	0.077	6.3×10^{12}	0.00014	0.01131	0.00029	1.0×10^{-5}	7	157	24	1.81	304	59

All fluid compositions have been calculated using the MRK equation of state of Holloway (1977) modified by Flowers (1979) and P, T, fO_2, fH_2O and fS_2 values listed in Table 1.

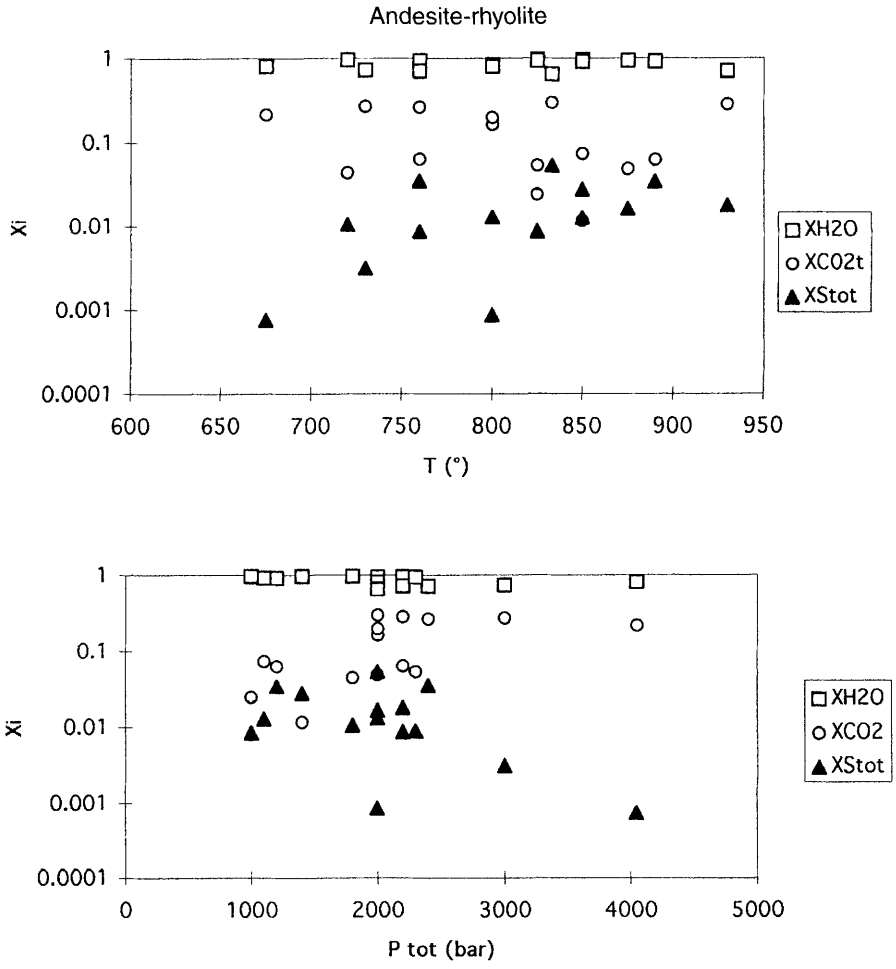

Fig. 5. Variation of the composition (X_i, mole fraction) of the pre-eruptive fluid phase with temperature and pressure in silicic to andesitic magmas.

than 0.6. Carbon dioxide is the second species in terms of molar abundance, with XCO_2 ranging between about 0.3 and 0.01. Other C-bearing species have concentrations 2 to 10 orders of magnitude lower than CO_2. In general XH_2S is the dominant S-bearing species, except in high-temperature oxidized magmas where XSO_2 equals or slightly exceeds XH_2S. The mole fraction of S_{tot} (XH_2S+XSO_2) approaches in some instances that of CO_2, but decreases significantly at temperatures below 750 °C (Fig. 5). Apart from this feature, the fluid composition is relatively insensitive to the pre-eruption temperature. The fluid becomes more CO_2-rich and H_2O- and S-poorer with pressure (Fig. 5), although there is a significant dispersion at around 2 kbar.

The compositional range displayed by pre-eruptive fluids can be conveniently described using C/S, H/S and H/C atomic ratios (Fig. 6). Pre-eruptive C/S ratios fall mostly in the range 1–10, while H/S ratios cluster around 100 except for some low-temperature magmas (Taupo, Pine Grove) that display higher values in both ratios due to their exceedingly low melt S contents. The fluid has H/C ratios almost always below 100 (Fig. 6). The comparison between the atomic ratios in both melt and fluid shows clearly that both phases differ significantly in terms of their H–C–S composition. Melts have lower C/S and higher H/S ratios, with the former being below 1 and the latter around 1000. Similarly, in the H/C v. C/S diagram, the two groups define a single trend but with no overlap. This contrasting

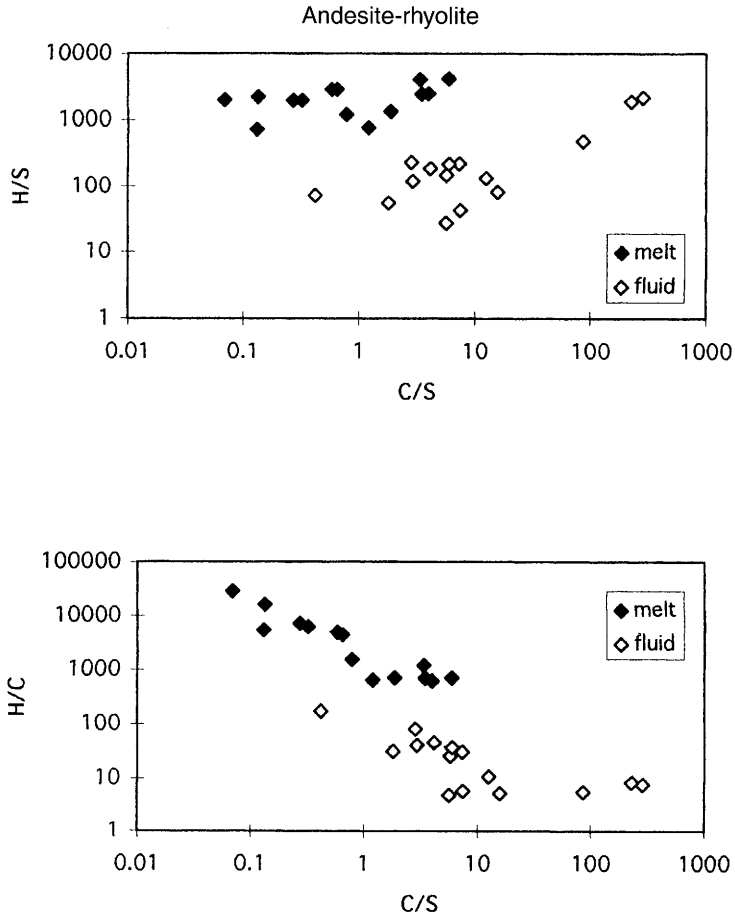

Fig. 6. Atomic compositions of pre-eruptive fluid (open symbols) and melt (closed symbols) phases in silicic to andesitic magmas.

behaviour is obviously due to the preferential partitioning of C- and S-bearing volatiles into the fluid phase. This phenomenon is best illustrated using partition coefficients for the major volatile species H_2O, CO_2 and S (Fig. 7). The three partition coefficients again show no obvious dependence on temperature, being fairly constant, with averages of $DH_2O=14$, $DS=257$ and $DCO_2=2268$. In contrast, all three partition coefficients decrease gently with pressure (Fig. 7), a trend that reflects the increasing solubilities of volatiles in silicate melts as pressure increases. When plotted against log fO_2, the S partition coefficients show no clear dependence on redox state. In particular, the partition coefficient calculated for the most reduced magma of the data-set (Santa Maria) appears to be similar to that obtained for other more oxidized magmas. This is in contrast with the experimental findings of Scaillet *et al.* (1998*b*) that suggest that the partition coefficients of sulphur in low fO_2 dacitic magmas are in the range 1–10. A possible explanation could be that the chosen pressure for the calculation, which has been fixed arbitrarily at 2 kbar, is too low. Amphiboles in Santa Maria dacite lavas are Al_2O_3-rich (11 wt%; Rose 1987), which could be explained by crystallization under higher pressures than the assumed 2 kbar. Calculations performed at 4 kbar yield a partition coefficient of 89 (instead of 321) which illustrates the sensitivity to pressure. Another possible source of error concerns the pre-eruptive melt sulphur content. If, instead of 198 ppm, a value of 100 ppm is taken, the corresponding S partition coefficient drops from 321 to 82. Although we have considered this

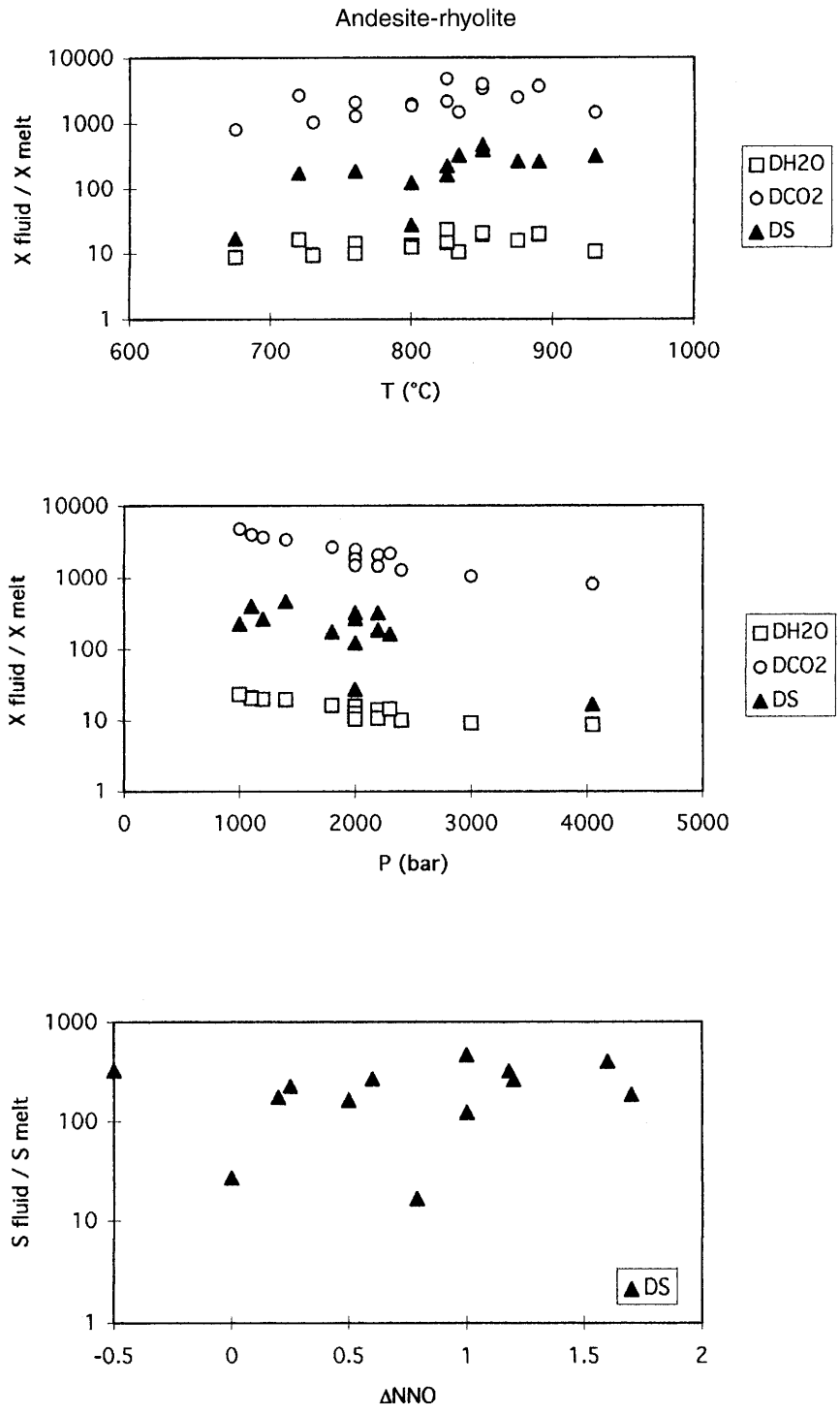

Fig. 7. Variation of the partition coefficients D of H_2O, CO_2 and S between fluid and melt (in wt%) with temperature, pressure, and fO_2 in silicic to andesitic magmas.

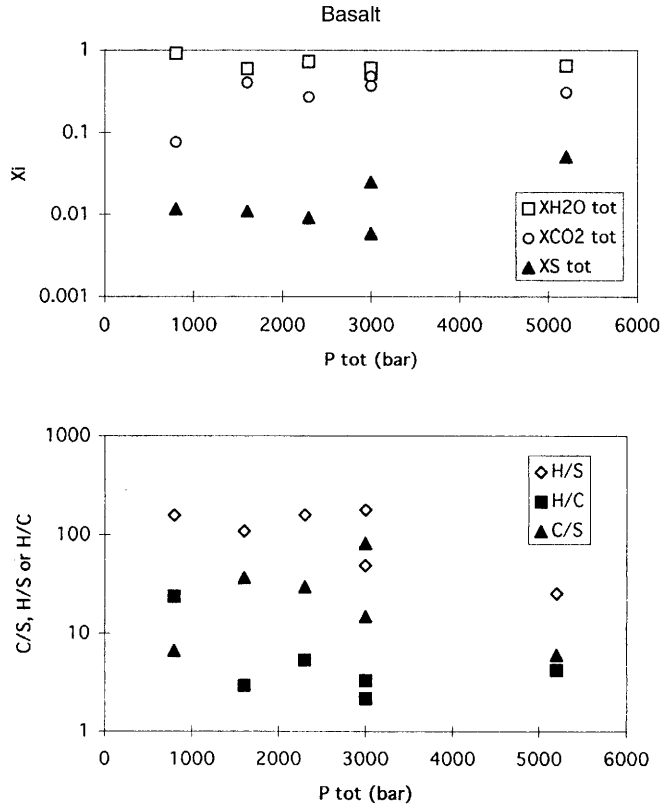

Fig. 8. Variation of the fluid phase composition with pressure (mole fraction of H_2O, CO_2, and S_{tot}, and atomic ratios) in basaltic magmas.

eruption because it allows us to extend the dataset to low fO_2 conditions, the disagreement between experimental and calculated S partition coefficients emphasizes the need for additional experimental work on the partitioning of sulphur between melt and coexisting fluid.

Mafic melt compositions

The calculated fluid phase compositions at equilibrium with mafic melt compositions are listed in Table 2. Compared with silicic to andesitic magmas, the fluid phase compositions display higher mole fractions of CO_2. Only at pressures below 1 kbar does the fluid become significantly richer in H_2O relative to CO_2 (Fig. 8). As with the silicic to andesitic group, both the fluid and melt atomic compositions differ (Fig. 9), with C/S ratios being higher than 10 for pre-eruptive fluids and lower than one for the melts, while both phases have a similar H/S ratio of around 100. A negative correlation also appears in the C/S v. H/C projection, with fluids displaying lower (<100) H/C ratios than melts (>100) (Fig. 9). The partition coefficients show again a negative dependence on pressure but, in this case, H_2O and S display roughly similar behaviour (Fig. 10) with average partition coefficients of 24 and 13 respectively, whereas CO_2 is always the most strongly volatile species partitioned toward the fluid, with partition coefficients continuously increasing from 473 at 5.2 kbar up to 5139 at 0.8 kbar.

Comparison with volcanic gases

Having computed the equilibrium fluid composition under pre-eruptive conditions, it is now possible to evaluate how this fluid compares with volcanic gas compositions. We restrict the comparison to volcanic gases with equilibrium or collection temperatures higher than 500 °C, since these are the most likely to preserve a large magmatic component (Symonds *et al.* 1994). We

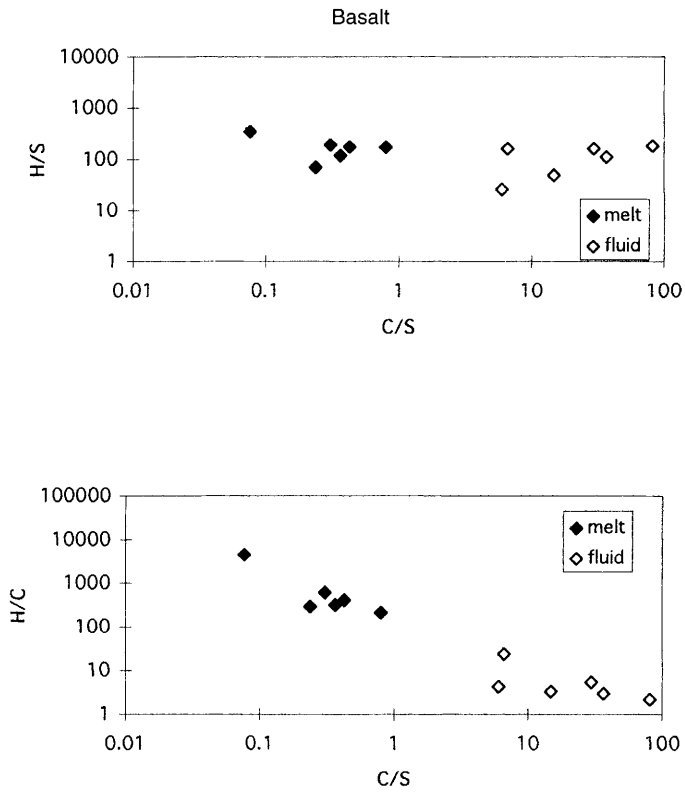

Fig. 9. Atomic compositions of pre-eruptive fluid (open symbols) and melt (closed symbols) phases in basaltic magmas.

use the recent compilation on convergent-plate volcanoes of Symonds *et al.* (1994), complemented by the additional recent data of Ohba *et al.* (1994), Fischer *et al.* (1998), Giggenbach *et al.* (2001), and Taran *et al.* (2001). Of the volcanic sites where gases have been sampled (Merapi, Unzen, St Helens, Showa–Shinzan, Usu, Kudryavi, Colima and Augustine for silicic to andesitic compositions, and Poas and Momotombo for basaltic ones) only two have their pre-eruption fluid composition constrained (Unzen and Mount St Helens). Therefore, a potential limitation of the following exercise results from the fact the volatile behaviour may change from site to site. Also (as stressed by Wallace 2001), for obvious reasons, the volcanic gases of explosive eruptions are extremely difficult to sample, whereas the estimates of pre-eruptive fluid compositions are based on tephra from the explosive phase. Nevertheless, as noted by many previous studies (e.g. Symonds *et al.* 1994), there are systematic trends in the analysed volcanic gas compositions of arc volcanoes, which presumably are of general significance.

Silicic to andesitic melt compositions

In terms of atomic ratios, volcanic gases display rather constant C/S ratios, mostly in the range 1–30, irrespective of temperature, while their H/S ratios show a general increase as temperature decreases (Fig. 11). High-temperature volcanic gases are extremely H_2O-rich, with XH_2O higher than 0.9, often in the range 0.95–0.99 (Fig. 12). The hottest gases, however, tend to be less H_2O-rich, with XH_2O dropping to near 0.8 (Fig. 12). The comparison with pre-eruptive fluids shows only partial overlap between the two groups, basically at high temperature (Fig. 12). A substantial proportion of volcanic gases are therefore not reproduced by equilibrium pre-eruptive fluids. A similar feature can be noted with respect to S. Both groups overlap at high temperature but, again, low-temperature

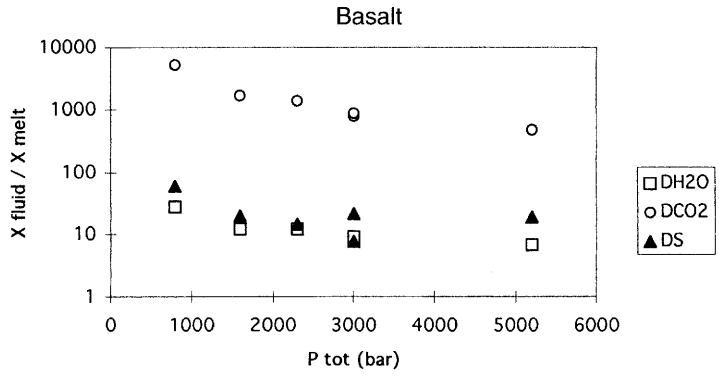

Fig. 10. Variation of the partition coefficients D of H_2O, CO_2 and S between fluid and melt (in wt%) with pressure in basaltic magmas.

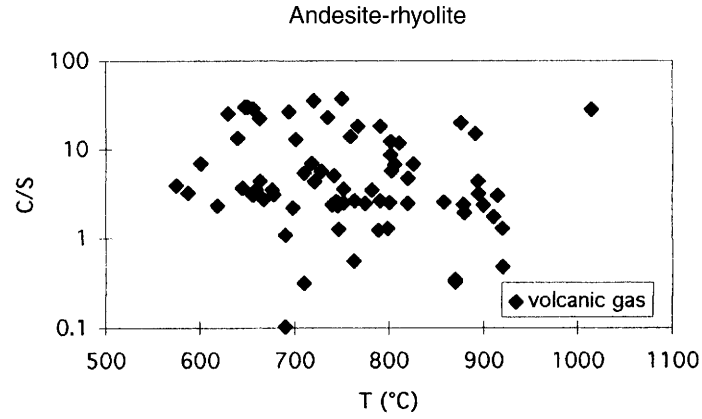

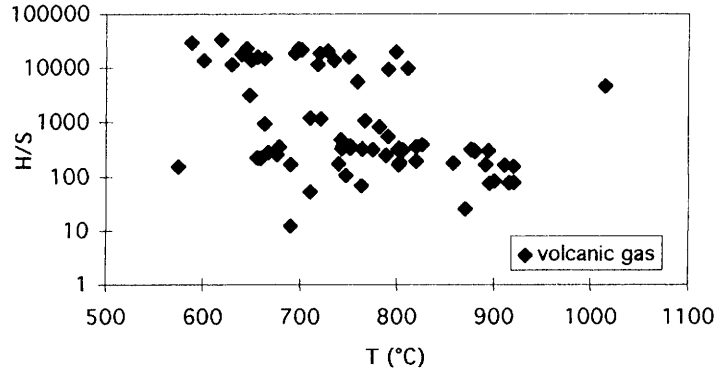

Fig. 11. Atomic compositions of volcanic gases v. temperature in silicic to andesitic volcanoes. See text for data sources.

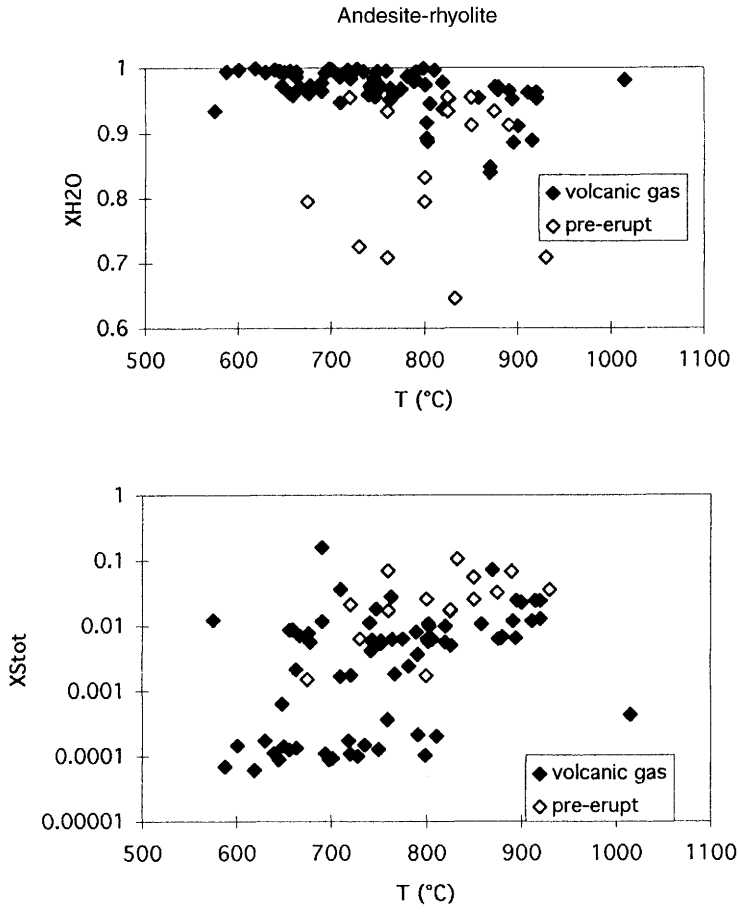

Fig. 12. Comparison of the mole fractions of H_2O and S_{tot} in volcanic gases (closed symbols) and pre-eruptive fluids (open symbols) v. temperature in silicic to andesitic volcanoes. See text for data sources.

volcanic gases tend to be much less S-rich than pre-eruptive ones (Fig. 12). Therefore, although both volcanic gas and pre-eruptive fluid display significant overlap in terms of their atomic compositions, the former show a conspicuous H_2O-enrichment trend, with H/C and H/S ratios notably higher than those calculated for the fluid at storage conditions (Fig. 13).

Mafic melt compositions

The compositional difference between pre-eruptive fluids and volcanic gases is even more apparent in basaltic systems, with no overlap between the two groups (Fig. 14). Although this gap could be due to the restricted number of gas analyses available, such a feature is due to the CO_2-rich character of pre-eruptive fluids in mafic arc magmas relative to those coexisting with more acid magmas (Table 2). High CO_2 contents shift C/S and H/C ratios to higher and lower values, respectively, relative to the coexisting melt.

The origin of the difference

There are two end-member cases for modelling the degassing processes that affect a magma at depth or during its ascent towards the surface. Degassing can occur with continuous separation of each increment of fluid phase generated from the magma and such that open system degassing takes place. Alternatively, degassing can occur *in situ*, in a closed system, with no separation between the degassing melt and the fluid phase, until perhaps the very late stage of the process, such as during an explosive eruptive event (see Villemant *et al.*, 2003, Chapter 5). Hydrogen isotope studies have shown that both types of

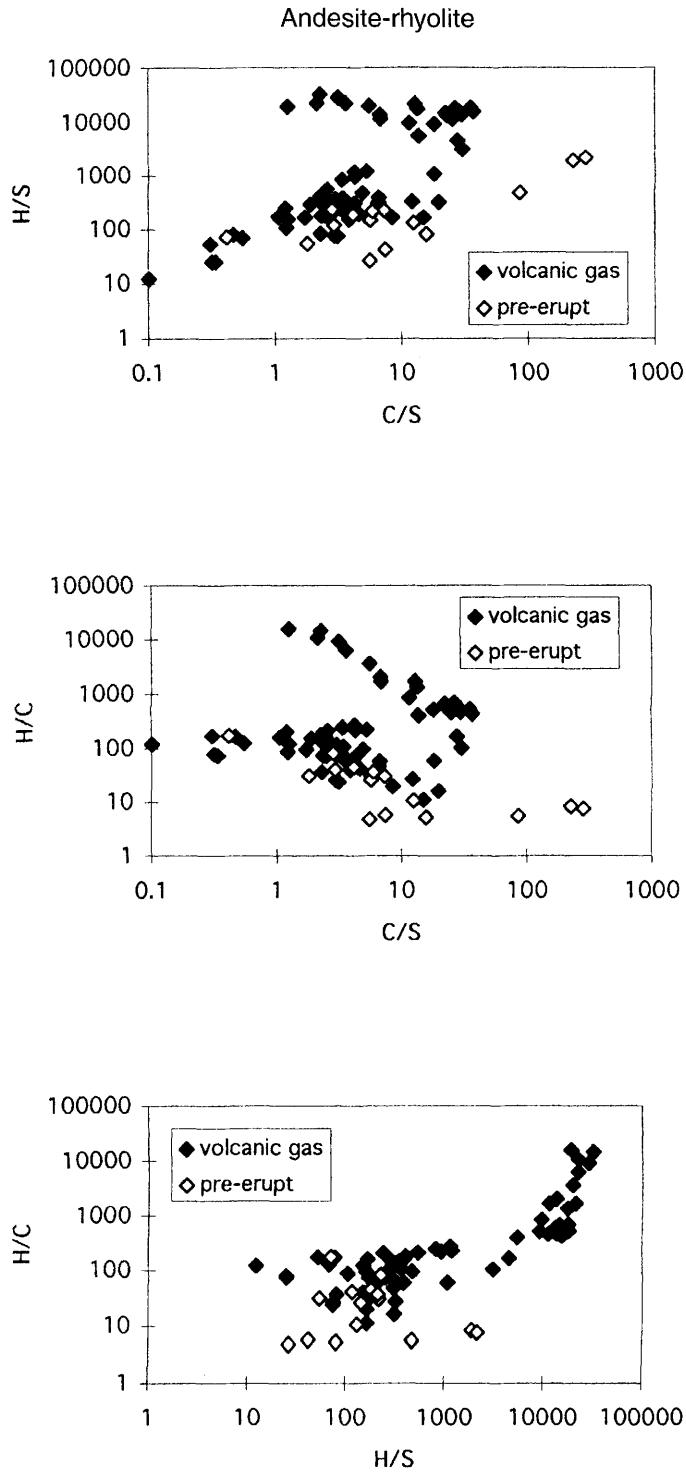

Fig. 13. Atomic composition of volcanic gases (closed symbols) and pre-eruptive fluids (open symbols) in silicic to andesitic magmas. See text for data sources.

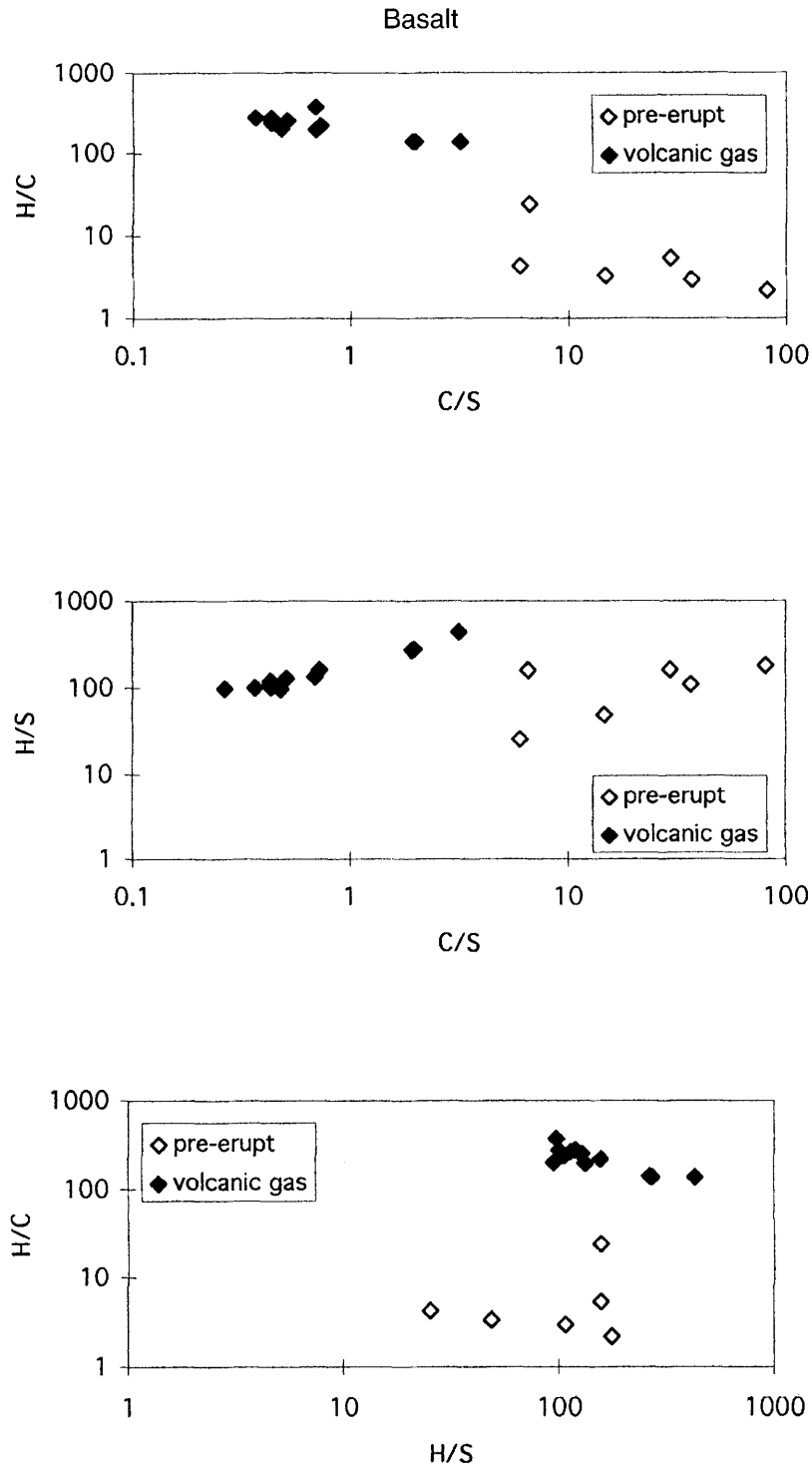

Fig. 14. Atomic composition of volcanic gases (closed symbols) and pre-eruptive fluids (open symbols) in basaltic magmas.

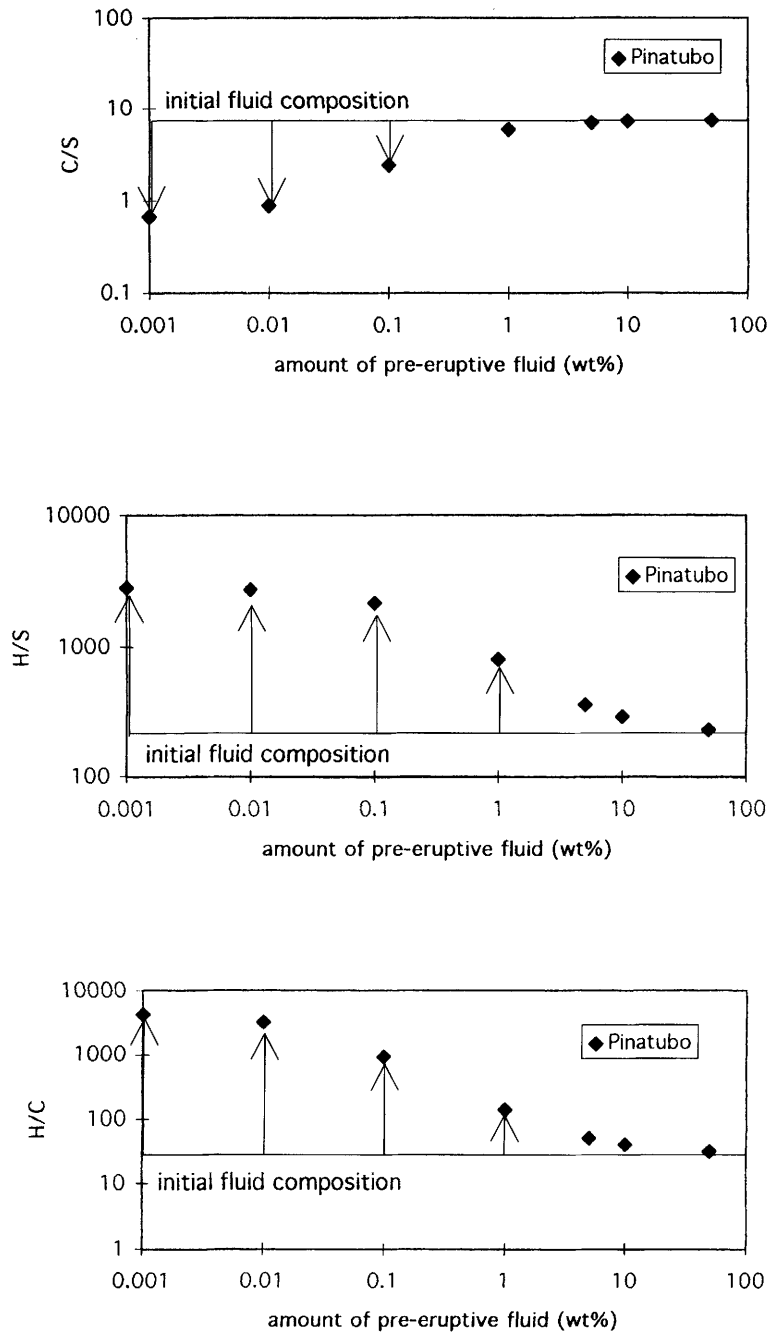

Fig. 15. Evolution of C/S, H/S and H/C atomic ratios of volcanic gases v. the amount of pre-eruptive fluids for the Pinatubo magma, calculated assuming closed-system behaviour. The horizontal lines represent the atomic ratio of the pre-eruptive fluid. Vertical arrows represent the change in atomic ratio followed by the exsolving fluid upon decompression to near-surface conditions, calculated for amounts of pre-eruptive fluid varying between 50 and 0. 001 wt%. See text for additional explanations. Magmas having amounts of pre-eruptive fluid lower than 1 wt% yield atmospheric fluid compositions significantly different from that in the deep reservoir.

degassing occur in silicic magmas (Taylor *et al.* 1983). The contrasted atomic compositions of both fluid and melt phases at depth offer a simple test for the closed-system scenario. In such a case, the final or exit fluid composition will depend on the storage conditions that fix both the compositions of melt and fluid, if any, and on the respective mass proportions of the two phases, according to the following simple mass-balance relations:

$$H_2O_{tot} = aH_2O_{melt} + bH_2O_{fluid} \quad (5)$$

$$CO_{2tot} = aCO_{2\ melt} + bCO_{2\ fluid} \quad (6)$$

$$SO_{2tot} = aSO_{2melt} + bSO_{2\ fluid} \quad (7)$$

with a and b being the mass fractions of the melt and fluid phases (taking into account the crystal content of the magma), and H_2O_{melt} and H_2O_{fluid} are the mass fractions of H_2O in melt and fluid, respectively (the same for CO_2 and SO_2). For the fluid we assume that $H_2O_{fluid} = H_2O + H_2$, $CO_{2\ fluid} = CO_2 + CO + CH_4$ and $SO_{2\ fluid} = SO_2 + H_2S + S_2$.

Calculations performed on the 1991 Pinatubo eruption illustrate the general evolution of C/S, H/S and H/C fluid atomic ratios following complete degassing (that is the final pressure is 1 bar, at which the H_2O, CO_2 and S solubilities are assumed to be close to zero), for a magma starting with different initial, i.e. pre-eruptive, amounts of fluid phase (Fig. 15). Physically, the calculations reproduce the hypothetical case of a decompressing melt+crystals+fluid mixture in which the melt continuously exsolves its C–O–H–S volatiles into a coexisting fluid phase that remains in contact with the magma until near-surface conditions are reached. As shown for the Pinatubo case, all three ratios undergo dramatic changes during decompression that are not linearly correlated with the initial amount of the fluid phase. The final C/S ratio of the fluid decreases by an order of magnitude if the magma at depth contains significantly less than 1 wt% (i.e. 0.1 wt%) of coexisting fluid phase. In contrast, pre-eruptive amounts of fluid higher than 1 wt% produce a marginal effect on the C/S ratio of the final fluid. In other words, as soon as the magma contains more than 1 wt% pre-eruptive fluid, the final fluid composition (assuming closed-system degassing) is essentially buffered by the starting composition of the fluid phase. The other atomic ratios display similar behaviour, yet the buffered condition is reached for higher amounts of pre-eruptive fluids, closer to 10 wt% (Fig. 15). The results of these simulations are shown for the evolution of the C/S ratio for three well-known eruptions in addition to Pinatubo (Bishop, St Helens and El Chichón). All four systems show the similar pattern of rapid increase in C/S for the first increments of pre-eruptive fluid, with the small inter-sample variations depending on the storage conditions and on the amount of crystallization, which in turn control the mass contribution of melt degassing to the fluid. Therefore, for andesitic to silicic magmas, a pre-eruptive fluid-saturated magma seems to be a necessary condition to reproduce the observed C/S ratios of volcanic gases (Fig. 11), if closed-system degassing holds.

Table 3 lists the results obtained for the silicic

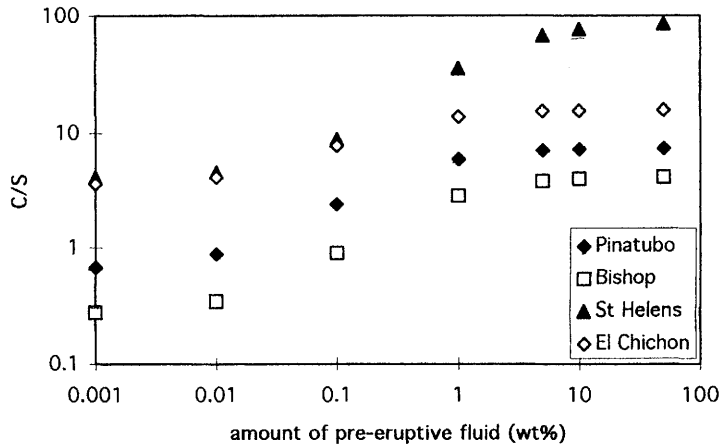

Fig. 16. Evolution of the C/S atomic ratios of volcanic gases v. the amount of pre-eruptive fluids for the Pinatubo, Bishop, St Helens and El Chichón magmas, calculated assuming closed-system behaviour.

Table 3. *Calculated volcanic gas compositions of arc volcanoes*

	XH_2O_{tot}	XCO_{2tot}	XS_{tot}	C/S	H/S	H/C
Silicic to andesitic compositions, 1 wt% pre-eruptive fluid						
Pinatubo	0.95672	0.03788	0.00541	7	355	51
Bishop	0.97250	0.02179	0.00571	4	343	90
Toba	0.87423	0.12393	0.00184	67	950	14
St Helens	0.83241	0.15742	0.01033	15	162	11
Krakatau	0.94546	0.03447	0.02044	2	94	55
El Chichón	0.88381	0.10714	0.00909	12	196	17
Fish Canyon	0.83465	0.14560	0.02020	7	84	12
Mt Pelée	0.95853	0.03075	0.01076	3	180	63
Montserrat	0.97455	0.00742	0.01823	0	109	267
Mt Unzen	0.93999	0.05095	0.00910	6	207	37
Crater Lake	0.80306	0.13361	0.06819	2	25	13
Taupo	0.90728	0.09206	0.00066	139	2738	20
Pine Grove	0.90089	0.09852	0.00060	165	3019	18
Katmai	0.98117	0.01367	0.00517	3	381	144
Santa Maria	0.77826	0.18775	0.03403	6	48	9
Minoan	0.97020	0.02518	0.00463	5	421	77
Basaltic compositions, 0.1 wt% pre-eruptive fluid						
Parent	0.96223	0.00971	0.02806	0.3	69	198
Cerro Negro	0.96124	0.01608	0.02267	0.7	85	120
Cerro Negro	0.95560	0.01122	0.03318	0.3	58	170
Cerro Negro	0.97176	0.00752	0.02072	0.4	94	258
Cerro Negro	0.96499	0.01267	0.02235	0.6	86	152
Cerro Negro	0.98569	0.00267	0.01165	0.2	169	740

to andesitic magma data-set with 1 wt% fluid under pre-eruptive conditions. In Figure 17, the results of the calculations performed for all magmas coexisting either with 1 wt% or 0.001 wt% fluid in the storage region are shown on a H/S v. H/C diagram. Clearly, again, the presence of 1 wt% fluid helps bridge the gap between volcanic gas compositions and the pre-eruptive compositions. It is also apparent that if the magmas were not fluid-saturated – a situation that is approached with the 0.001 wt% fluid condition, then the final fluid phase would lie clearly outside the field of observations. Yet, there is still a significant portion of the field delimited by natural gases – the H/C- and H/S-rich apex of the domain – that is not reproduced by the simulation. As shown previously, most of these are H_2O-rich, S-poor and low-temperature gases. Possible explanations for the origin of these H_2O-rich and S-poor fluids are that: (1) the colder volcanic gases have been contaminated by meteoric waters; (2) precipitation of C- and S-bearing minerals has altered the original magmatic fluid during cooling; (3) degassing cannot be modelled as a closed system; or (4) the process of segregation of fluid from melt is not an equilibrium one – such that kinetic factors control the composition of the fluid. In particular, it is well known that both S- and C-bearing volatiles are slow-diffusing species in silicate melts as compared with H_2O which has a diffusivity many orders of magnitude higher than those of S and CO_2 (Watson 1994). This could lead to a selective enrichment in H over S and C during ascent-controlled degassing.

The same simulations have been performed for the mafic data-set and are displayed in Figure 17. The results of calculations for a magma having 0.1 wt% fluid at depth are listed in Table 3. In contrast to silicic–andesitic systems, the simulation nearly perfectly reproduces the natural gas compositional field, and it does so when the magmas coexist with 0.1–1 wt% fluid at depth. Interestingly, the amount of pre-eruptive fluid needed to reproduce the volcanic gas composition is roughly pressure-dependent –being higher at low pressure. For instance, the melt inclusion with an entrapment pressure of 800 bar requires 1 wt% fluid to join the volcanic gas field, while that entrapped at 5.2 kbar needs only 0.1 wt%. To a first approximation, this is in agreement with the fact that, as a volatile-bearing magma decompresses as a closed system, the amount of coexisting fluid must increase. Calculation in the simple basalt–H_2O system shows that at 5 kbar a basaltic magma at H_2O–saturation has about 8.6 wt% H_2O in solution (see Dixon *et al.* 1995). If it

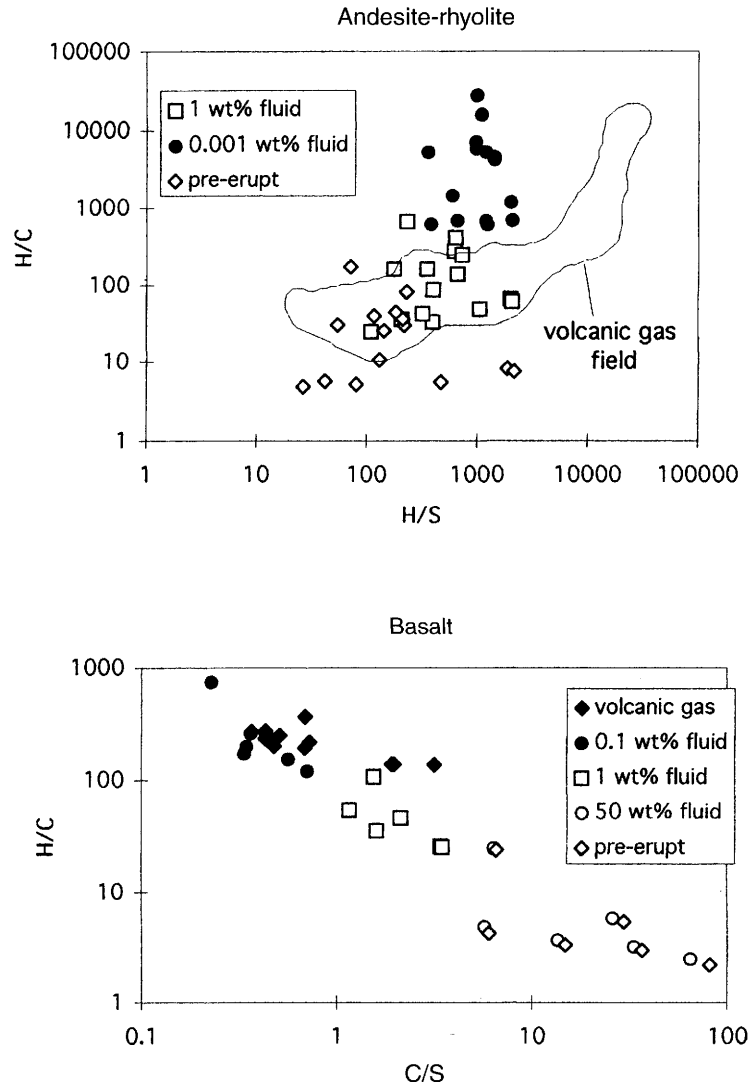

Fig. 17. H/S v. H/C plot showing the effect of the amount of pre-eruptive fluid on the final volcanic gas composition, calculated assuming closed-system behaviour. The calculations are shown for 1 and 0.001 wt% fluid (silicic to andesitic magmas) and 50, 1 and 0.1 wt% fluid (basaltic magmas).

decompresses to 800 bar, where the solubility is only 2.9 wt% H_2O, then it will coexist with 6 wt% fluid, in substantial agreement with our estimate.

Discussion and conclusions

The comparison between calculated fluid phase chemistries under pre-eruptive conditions and volcanic gases shows overall good agreement. This suggests that thermodynamic models of volatile solubilities in silicic to mafic melts and their coexisting fluids are reasonably well calibrated, with good predictive capabilities at *P–T* conditions relevant to arc-magma genesis and evolution. It seems clear that silicic to andesitic magmas coexist with fluid at depth, in agreement with a number of independent lines of evidence (Anderson *et al.* 1989; Westrich & Gerlach 1992; Wallace *et al.* 1995; Gerlach *et al.* 1996; Scaillet *et al.* 1998*b*; Wallace 2001). The

overlap between pre-eruptive fluid and volcanic gas compositions indicates that, in some instances, this pre-eruptive fluid may escape the reservoir and reach the surface unaltered. Yet, most volcanic gas compositions require a contribution from melt degassing at low pressure. For this to be possible, a physical contact between melt and fluid, or absence of significant segregation, is required over a significant portion of the ascent path. One possible reason lies in the viscous character of the residual melt of most silicic to andesitic magmas, which significantly inhibits fluid fractionation, especially in situations where magma ascent takes place over short time-scales. There is also a population of volcanic gases that is not reproduced by the simple calculations performed in the present paper. The fact that they are, in general, the colder gases, with equilibrium temperatures below the solidus temperatures of any arc magmas (<650 °C), suggests that they may have been significantly modified before collection, such as through interaction with low-temperature hydrothermal fluids. Precipitation of S-bearing minerals during cooling may be an obvious alternative or additional mechanism to remove sulphur from the fluid.

For mafic melt compositions, the amount of pre-eruptive fluid required to reproduce volcanic gases is smaller than for silicic compositions, which is in qualitative agreement with the highly differentiated nature of andesitic to silicic magmas, but clearly there is a need for additional data concerning the volatile contents of mafic arc magmas. The available data point to the existence of two separate trends in the T–H_2O diagram (Fig. 4), which need further discussion. The fact that the high-temperature end of the silicic–andesite trend plots significantly below the low-temperature end of the mafic trend merely reflects the fact that the studied basalt magmas were stored at higher pressures, and thus could reach higher water contents than the more silicic ones. Andesites produced by fractionation of hydrous basalts at around 4 kbar, such as in the Lesser Antilles arc (Pichavant *et al.* 2002*a*), must be fluid-saturated during nearly all their evolution, since their parental basaltic magma starts crystallizing with H_2O contents, at 4 kbar, of 6–8 wt% (Pichavant *et al.* 2002*a*), i.e. close to or even higher than the solubility value at 2–3 kbar. Still, near-liquidus and H_2O-rich andesitic magmas (i.e. at 950 °C and with 6 wt% H_2O) have yet to be sampled. As for H_2O-rich basalts, this absence could indicate that those magmas cannot erupt without massive, decompression-driven, crystallization. In fact, heavily crystallized andesitic magmas near H_2O-saturation seem more common, as illustrated by the Mount Pelée and Montserrat eruptions. In such cases, the magma column feeding the volcano is likely to be fluid-saturated over a substantial depth interval. The evidence summarized above suggests that magma degassing may start at pressures as high as 4 kbar, and not just very late at shallow levels during eruption or within the roof of an upper-crustal reservoir, as was commonly believed.

How this continuous degassing may affect the fluid chemistry and the residual melt still remains to be quantitatively evaluated. However, this is not to say that arc-basalts inevitably stall and fractionate at around 4 kbar, and that all andesite magmas are fluid-saturated. There are certainly many instances, especially during the less-mature stage of arc development where the crust is thinned, in which basalt storage occurs at 2 kbar, or at even lower pressures. Were analytical or experimental data available for such occurrences, they would presumably extend the silicic–andesitic trend toward higher temperatures (see Fig. 4). Similarly, there are andesite occurrences whose pre-eruptive melt water content seems to deviate significantly from saturation values (i.e. the andesite at Katmai if the storage pressure is 2 kbar). This suggests that the degree of H_2O-enrichment in arc magmas, whether mafic or felsic, may vary greatly for both intra- and inter-arc situations.

As previously noted, the weak dependence of S melt contents on fO_2 suggests that fO_2 exerts little control on the sulphur solubility in natural magmas. While this might appear surprising, it mainly reflects the fact that the fS_2 values displayed by natural magmas are in the range where fO_2 control on S solubility is minor (Fig. 1). Maintaining low fS_2 in natural magmas can be achieved through two main mechanisms:

1. Under reduced conditions, the S solubility is controlled via sulphide–melt equilibrium, as discussed by Wallace and Carmichael (1992). The great affinity between iron and sulphur under reduced conditions is a well-established feature, as indicated by the strong positive correlation between the two elements. Despite this affinity, reduced basaltic magmas cannot dissolve large amounts of S, because they soon develop an immiscible sulphide melt which prevents the magma from reaching excessive values, say several bars, of fS_2. Experimental data and theoretical modelling show that natural, sulphide-saturated, basaltic melts have fS_2 generally below 1 bar, corresponding with S melt contents in the order of 1300 ppm (Wallace & Carmichael 1992), apart from some Fe–Ti-rich basalts, which

can have up to 2500 ppm dissolved sulphur (P. Wallace, pers. comm.).

2. Under oxidizing conditions, such as in arc magmas, fluid–melt equilibrium can be an additional controlling factor of the S concentration of the melt, along with solid–melt or melt–melt equilibria. If the amount of pre-eruptive fluid in arc magmas is in the range 1–6 wt% (e.g. Wallace 2001), then most of their sulphur content will be stored in the fluid phase. Indeed, calculated sulphur contents of pre-eruptive fluids are mostly in the range 1–6 wt% S (Table 2), except for low-temperature and reduced silicic magmas. Ignoring the potential contribution of pyrrhotite and anhydrite, a magma with 5 wt% fluid that is half crystallized, with a residual melt S content of 100 ppm, has more than 98.4% of its bulk sulphur stored in the fluid if the latter contains 6 wt% S (91.4% for 1 wt% S in fluid). The fluid phase may therefore effectively buffer the S content of the melt of arc magmas, at least for silicic compositions. It should not be concluded, however, that fO_2 does not affect the sulphur behaviour at all. Clearly, fO_2 will fix the S^{2-}/S^{6+} ratio (Carroll & Webster 1994), but the bulk S content of the melt appears to be controlled by the coexisting fluid phase, otherwise natural magmas should display a pronounced depletion in their S content in the fO_2 range NNO – NNO+1, a trend not observed.

From the standpoint of experimental petrology, the present study shows that additional work is needed for the accurate determination of partition coefficients of S using an experimental procedure where both the fluid and melt have their S contents determined. The determination of the relationships between fS_2 and S in hydrous basaltic melts is another important task if rigorous modelling of the evolution of the fluid phase in hydrous mafic systems is to be attempted. The dependence on P_{tot} of S solubility in both mafic and silicic melts also remains to be evaluated. Finally, in recent years, much effort has been put into measuring Cl solubility and partitioning in felsic to mafic melts (Carroll & Webster 1994; Webster *et al.* 1999), the reason being that many arc magmas display significant Cl concentrations. Studies aimed at quantifying the relationships between fHCl and Cl solubility would therefore be highly valuable.

This paper greatly benefited from helpful reviews of P. Wallace and C. Mandeville, and from the editorial intervention of C. Oppenheimer. J. Lowenstern kindly supplied critical information on pre-eruptive conditions for the Pine Grove eruption. Numerous discussions with F. Costa helped to improve the manuscript.

References

ANDERSON, A. T., NEWMAN, S., WILLIAMS, S. N., DRUITT, T. H., SKIRIUS, C. & STOLPER, E. 1989. H_2O, CO_2, Cl gas in Plinian and ash-flow Bishop rhyolite. *Geology*, **17**, 221–225.

BLAKE, S. 2003. Correlations between eruption magnitude, SO_2 yield and surface cooling. *In:* OPPENHEIMER, C., PYLE, D.M. & BARCLAY, J. (eds) *Volcanic Degassing.* Geological Society, London, Special Publications, **213**, 371–380.

BLANK, J. G., STOLPER, E. M., & CARROLL, M. R. 1993. Solubilities of carbon dioxide and water in rhyolitic melts. *Earth and Planetary Science Letters*, **119**, 27–36.

CARROLL, M. R. & WEBSTER, J. D. 1994. Solubilities of sulfur, noble gases, nitrogen, chlorine and fluorine in magmas. *In*: CARROLL, M. R. & HOLLOWAY, J. R. (eds) *Volatiles in Magmas*, Reviews in Mineralogy, **30**, 231–279.

CHOU, I. M. 1987. Oxygen buffer and hydrogen sensor technique at elevated pressures and temperatures. *In:* BARNES, H. L. & ULMER, G. C. (eds) *Hydrothermal Experimental Techniques*. John Wiley, New York, 61–99.

CLEMENTE, B., SCAILLET, B. & PICHAVANT, M. 2003. The solubility of sulphur in rhyolite. *Journal of Petrology* (in press).

COOMBS, M. L. & GARDNER, J. E. 2001. Shallow-storage conditions for the rhyolite of the 1912 eruption at Novarupta, Alaska. *Geology*, **29**, 775–778.

COTTRELL, E., GARDNER, J. & RUTHERFORD, M. J. 1999. Petrologic and experimental evidence for the movement and heating of the pre-eruptive Minoan rhyodacite (Santorini, Greece). *Contributions to Mineralogy and Petrology*, **135**, 315–331.

DIXON, J. E., STOLPER, E. M. & HOLLOWAY, J. R. 1995. An experimental study of water and carbon dioxide solubilities in mid-ocean ridge basaltic liquids. Part I: calibration and solubility models. *Journal of Petrology*, **36**, 1607–1631.

FISCHER, T. P., MORRISSEY, M. M., CALVACHE, M. L., DIEGO GOMEZ, M., ROBERTO TORRES, C., STIX, J. & WILLIAMS, S. N. 1994. Correlations between SO_2 flux and long period seismicity at Galeras volcano. *Nature* **368**, 135–137.

FISCHER, T. P., GIGGENBACH, W. F., SANO, S. & WILLIAMS, S. N. 1998. Fluxes and sources of volatiles discharged from Kudryavy, a subduction zone volcano, Kurile Islands. *Earth and Planetary Science Letters*, **160**, 81–96.

FLOWERS, G. C. 1979. Correction of Holloway's (1977) adaptation of the Modified Redlich–Kwong equation of state for calculation of the fugacities of molecular species in supercritical fluids of geologic interest. *Contributions to Mineralogy and Petrology*, **69**, 315–318.

FROESE, E. & GUNTER, A. E. 1976. A note on the pyrrhotite–sulfur vapor equilibrium. *Economic Geology*, **71**, 1589–1594.

GERLACH, T. M., WESTRICH, H. R. & SYMONDS, R. B. 1996. Pre-eruption vapor in magma of the climactic Mount Pinatubo eruption: source of the giant stratospheric sulfur dioxide cloud. *In:* NEWHALL, C. G. & PUNONGBAYAN, R. S. (eds) *Fire and Mud. Eruptions and Lahars of Mount Pinatubo, Philippines,* University of Washington Press, 415–434.

GIGGENBACH, W. F., TEDESCO, D. ET AL. 2001. Evaluation of results from the fourth and fifth IAVCEI field workshops on volcanic gases, Vulcano island, Italy and Java, Indonesia. *Journal of Volcanology and Geothermal Research*, **108**, 157–172.

HOLLOWAY, J. R. 1977. Fugacity and activity of molecular species in supercritical fluids. In: FRASER, D. (ed.) *Thermodynamics in Geology*. Riedel, Dordrecht, 161–181.

HOLLOWAY, J. R. & BLANK, J. 1994. Applications of experimental results to C–O–H species in natural melts. *In:* CARROLL, M. R. & HOLLOWAY, J. R. (eds) *Volatiles in Magmas*, Reviews in Mineralogy, **30**, 187–230.

JOHNSON, M. C. & RUTHERFORD, M. J. 1989. Experimentally determined conditions in the Fish Canyon Tuff, Colorado, magma chamber. *Journal of Petrology*, **30**, 711–737.

JOHNSON, M. C., ANDERSON, A. T. & RUTHERFORD, M. 1994. Pre-eruptive volatile contents of magmas. *In:* CARROLL, M. R. & HOLLOWAY, J. R. (eds), *Volatiles in Magmas*, Reviews in Mineralogy, **30**, 281–330.

KEPPLER, H. 1999. Experimental evidence for the source of excess sulfur in explosive volcanic eruptions. *Science* **284**, 1652–1654.

LUHR, J. F. 1990. Experimental phase relations of water- and sulfur-saturated arc magmas and the 1982 eruptions of El Chichón volcano. *Journal of Petrology*, **31**, 1071–1114.

LUHR, J. F. 2001. Glass inclusions and melt volatile contents at Paricutin volcano, Mexico. *Contributions to Mineralogy and Petrology* **142**, 261–283.

MCGONIGLE, A. & OPPENHEIMER, C. 2003. Optical sensing of volcanic gas and aerosol emissions. *In:* OPPENHEIMER, C., PYLE, D. M. & BARCLAY, J. (eds) *Volcanic Degassing*. Geological Society, London, Special Publications, **213**, 149–168.

MANDEVILLE, C. W., CAREY, S. & SIGURDSSON, H. 1996. Magma mixing, fractional crystallisation and volatile degassing during the 1883 eruption of Krakatau volcano, Indonesia. *Journal of Volcanology and Geothermal Research*, **74**, 243–274.

MARTEL, C. 1996. Conditions pré-éruptives et dégazage des magmas andésitiques de la Montagne Pelée (Martinique): étude pétrologique et expérimentale. Unpublished PhD thesis, Université d'Orléans, 299 pp.

MARTEL, C., PICHAVANT, M., BOURDIER, J. L, TRAINEAU, H., HOLTZ, F. & SCAILLET, B. 1998. Magma storage conditions and control of eruption regime in silicic volcanoes: experimental evidence from Mt. Pelée. *Earth and Planetary Science Letters*, **156**, 89–99.

MARTEL, C., PICHAVANT, M., HOLTZ, F., SCAILLET, B., BOURDIER, J. L & TRAINEAU, H. 1999. Effects of fO_2 and H_2O on andesite phase relations between 2 and 4 kbar. *Journal of Geophysical Research*, **104**, 29 453–29 470.

MÉTRICH, N. & CLOCCHIATTI, R. 1996. Sulfur abundance and its speciation in oxidized alkaline melts. *Geochimica et Cosmochimica Acta*, **60**, 4151–4160.

MÉTRICH, N., SCHIANO, P., CLOCCHIATTI, R. & MAURY, R. C. 1999. Transfer of sulfur in subduction settings: an example from Batan Island (Luzon volcanic arc, Philippines). *Earth and Planetary Science Letters*, **167**, 1–14.

MICHAUD, V., CLOCCHIATTI, R. & SBRANA, S. 2000. The Minoan and post-Minoan eruptions, Santorini (Greece), in the light of melt inclusions: chlorine and sulphur behaviour. *Journal of Volcanology and Geothermal Research*, **99**, 195–214.

MORETTI, R., PAPALE, P. & OTTONELLO, G. 2003, A model for the saturation of C–O–H–S fluids in silicate melts. *In*: OPPENHEIMER, C., PYLE, D.M. & BARCLAY, J. (eds) *Volcanic Degassing.* Geological Society, London, Special Publications, **213**, 81–101.

OHBA, T., HIRABAYASHI, J. & YOSHIDA, M. 1994. Equilibrium temperature and redox state of volcanic gas at Unzen volcano, Japan. *Journal of Volcanology and Geothermal Research*, **60**, 263–272.

PALAIS, J. & SIGURDSSON, H. 1989. Petrologic evidence of volatile emissions from major historic and prehistoric volcanic eruptions. *In*: BERGER, A. L., DICKINSON, R. E. & KIDSON, J. (eds) *Understanding Climate Change*, AGU, Washington D.C., 31–53.

PICHAVANT, M., MARTEL, C., BOURDIER, J. L. & SCAILLET, B. 2002*a*. Physical conditions, structure and dynamics of a zoned magma chamber: Mt. Pelée (Martinique, Lesser Antilles arc). *Journal of Geophysical Research*, **107(B5),** 101029/2001JB-000315.

PICHAVANT, M., MYSEN, B. O. & MACDONALD, R. 2002*b*. Origin and H_2O content of high-MgO magmas in island arc settings: an experimental study of a primitive calc-alkaline basalt from St Vincent, Lesser Antilles Arc. *Geochimica et Cosmochimica Acta*, **66**, 2193–2209.

ROBIE, R. A., HEMINGWAY, B. S. & FISHER, J. R. 1979. *Thermodynamic Properties of Minerals and Related Substances at 298.15 K and 1 bar (10^5 pascals) Pressure and at Higher Temperature.* US Geological Survey Bulletin, **1452**, 456 pp.

ROBOCK, A. 2000. Volcanic eruptions and climate. *Reviews of Geophysics*, **38**, 191–219.

ROGGENSACK, K. 2001. Unraveling the 1974 eruption of Fuego volcano (Guatemala) with small crystals and their young melt inclusions. *Geology*, **29**, 911–914.

ROGGENSACK, K., HERVIG, R. L., MCKNIGHT, S. B. & WILLIAMS, S. N. 1997. Explosive basaltic volcanism from Cerro Negro volcano: influence of volatiles on eruptive style. *Science*, **277**, 1639–1642.

ROSE, W. I. 1987. Santa Maria, Guatemala: bimodal soda-rich calc-alkalic stratovolcano. *Journal of Volcanology and Geothermal Research*, **33**, 109–129.

ROSE, W. I., STOIBER, R. E. & MALINCONICO, L. L. 1982. Eruptive gas compositions and fluxes of

explosive volcanoes: budget of S and Cl emitted from Fuego volcano, Guatemala. *In*: Thorpe, R. S. (ed.) *Andesites*, John Wiley, London, 669–676.

RUTHERFORD, M. J., & DEVINE, J. D. 1988. The May 18, 1980 eruption of Mount St. Helens: 3, Stability and chemistry of amphibole in the magma chamber. *Journal of Geophysical Research*, **93**, 949–959.

RUTHERFORD, M. J. & DEVINE, J. D. 1996. Pre-eruption pressure–temperature conditions and volatiles in the 1991 Mount Pinatubo magma. *In:* NEWHALL, C. G. & PUNONGBAYAN, R. S. (eds) *Fire and Mud. Eruptions and Lahars of Mount Pinatubo, Philippines*, University of Washington Press, 751–766.

RUTHERFORD, M. J. & HILL, P. M. 1993. Magma ascent rates from amphibole breakdown: an experimental study applied to the 1980–1986 Mount St. Helens eruptions. *Journal of Geophysical Research*, **98**, 19 667–19 685.

RUTHERFORD, M. J., SIGURDSSON, H. & CAREY, S. 1985. The May 18, 1980 eruption of Mount St. Helens: 1, Melt composition and experimental phase equilibria. *Journal of Geophysical Research*, **90**, 2929–2947.

SATO, H., NAKADA, S., FUJII, T., NAKAMURA, M. & SUZUKI-KAMATA, K. 1999. Groundmass pargasite in the 1991–1995 dacite of Unzen volcano: phase stability experiments and volcanological implications. *Journal of Volcanology and Geothermal Research*, **89**, 197–212.

SCAILLET, B. & EVANS, B. W. 1999. The June 15, 1991 eruption of Mount Pinatubo. I. Phase equilibria and pre-eruption P–T–fO_2–fH_2O conditions of the dacite magma. *Journal of Petrology*, **40**, 381–411.

SCAILLET, B. & MACDONALD, R. 2001. Phase relations of peralkaline silicic magmas and petrogenetic implications. *Journal of Petrology*, **42**, 825–845.

SCAILLET, B., HOLTZ, F. & PICHAVANT, M. 1998*a*. Phase equilibrium constraints on the viscosity of silicic magmas 1. Volcanic–plutonic comparison. *Journal of Geophysical Research*, **103**, 27 257–27 266.

SCAILLET, B., CLEMENTE, B., EVANS, B. W. & PICHAVANT, M. 1998*b*. Redox control of sulfur degassing in silicic magmas. *Journal of Geophysical Research*, **103**, 23 937–23 949.

SILVER, L. A. & STOLPER, E. 1985. A thermodynamic model for hydrous silicate melts. *Journal of Geology*, **93**, 161–178.

SISSON, T. W. & BRONTO, S. 1998. Evidence for pressure–release melting beneath magmatic arcs from basalts at Galunggung, Indonesia. *Nature*, **391**, 883–886.

SISSON, T. W. & GROVE, T. L. 1993*a*. Experimental investigations of the role of H_2O in calc-alkaline differentiation and subduction zone magmatism. *Contributions to Mineralogy and Petrology* **113**, 143–166.

SISSON, T. W. & GROVE, T. L. 1993*b*. Temperatures and H_2O contents of low-MgO high alumina basalts. *Contributions to Mineralogy and Petrology* **113**, 167–184.

SISSON, T. W. & LAYNE, G. D. 1993. H_2O in basaltic and basaltic andesite glass inclusions from four subduction-related volcanoes. *Earth and Planetary Science Letters*, **117**, 619–635.

SOBOLEV, A. V. & CHAUSSIDON, M. 1996. H_2O concentrations in primary melts from supra-subduction zones and mid-ocean ridges: implications for H_2O storage and recycling in the mantle. *Earth and Planetary Science Letters*, **137**, 45–55.

SYMONDS, R. B., ROSE, W. I., BLUTH, G. J. S. & GERLACH, T. M. 1994. Volcanic gas studies: methods, results, and applications. *In:* CARROLL, M. R. & HOLLOWAY, J. R. (eds) *Volatiles in Magmas*, Reviews in Mineralogy, **30**, 1–60.

TARAN, Y. A., BERNARD, A., GAVILANES, J. C., LUNEZHEVA, E., CORTES, A. & ARMIENTA, M. A. 2001. Chemistry and mineralogy of high temperature gas discharges from Colima volcano, Mexico. Implications for magmatic gas–atmosphere interaction. *Journal of Volcanology and Geothermal Research*, **108**, 245–264.

TAYLOR, B. E., EICHELBERGER, J. C. & WESTRICH, H. R. 1983. Hydrogen isotopic evidence of rhyolitic magma degassing during shallow intrusion and degassing. *Nature*, **306**, 541–545.

TOULMIN III, P. & BARTON JR, B. P. 1964. A thermodynamic study of pyrite and pyrrhotite. *Geochimica et Cosmochimica Acta*, **28**, 641–671.

VILLEMANT, B., BOUDON, G., NOUGRIGAT, S., POTEAUX, S. & MICHEL, A. 2003 Water and halogens in volcanic clasts: tracers of degassing processes during plinian and dome-forming eruptions. *In*: OPPENHEIMER, C., PYLE, D.M. & BARCLAY, J. (eds) *Volcanic Degassing.* Geological Society, London, Special Publications, **213**, 63–79.

WALLACE, P. J. 2001. Volcanic SO_2 emissions and the abundance and distribution of exsolved gas in magma bodies. *Journal of Volcanology and Geothermal Research*, **108**, 85–106.

WALLACE, P. J. & CARMICHAEL, I. S. E. 1992. Sulfur in basaltic magmas. *Geochimica et Cosmochimica Acta* **56**, 1863–1874.

WALLACE, P. J. & GERLACH, T. M. 1994. Magmatic vapor source for sulfur dioxide released during volcanic eruptions: evidence from Mount Pinatubo, *Science*, **265**, 497–499.

WALLACE, P. J., ANDERSON, A. T. & DAVIS, A. M. 1995. Quantification of pre-eruptive exsolved gas contents in silicic magmas. *Nature* **377**, 612–615.

WATSON, E. B., 1994. Diffusion in volatile-bearing magmas. *In:* CARROLL, M. R. & HOLLOWAY, J. R. (eds) *Volatiles in Magmas.* Reviews in Mineralogy, **30**, 371–411.

WATSON, I. M. & OPPENHEIMER, C., *ET AL.* 2000. The relationship between degassing and ground deformation at Soufriere Hills Volcano, Montserrat. *Journal of Volcanology and Geothermal Research*, **98**, 117–126.

WEBSTER, J., KINZLER, R. J. & MATHEZ, E. 1999. Chloride and water solubility in basalt and andesite melts and implications for magmatic degassing. *Geochimica et Cosmochimica Acta*, **63**, 729–738.

WESTRICH, H. R. & GERLACH, T. M. 1992. Magmatic gas source for the stratospheric SO_2 cloud from the June 15, 1991 eruption of Mount Pinatubo. *Geology*, **20**, 867–870.

WHITNEY, J. A. 1984. Fugacities of sulfurous gases in pyrrhotite-bearing silicic magmas. *American Mineralogist*, **69**, 69–78.

ZHANG, Y. 1999. H_2O in rhyolitic glasses and melts: measurement, speciation, solubility, and diffusion. *Reviews of Geophysics*, **37**, 493–516.

ZIELINSKI, G. A. 1995. Stratospheric loading and optical depth estimates of explosive volcanism over the last 2100 years derived from the Greenland Ice Sheet Project 2 ice core. *Journal of Geophysical Research* **100**, 20 937–20 955.